Renewable and Sustainable Energy Reviews 133 (2020) 110100

Contents lists available at ScienceDirect

Renewable and Sustainable Energy Reviews

journal homepage: http://www.elsevier.com/locate/rser

Review of current progress in non-aqueous aluminium batteries

Ben Craig [a,**], Theresa Schoetz [b], Andrew Cruden [a], Carlos Ponce de Leon [a,*]

[a] Faculty of Engineering and Physical Sciences; Mechanical Engineering Department, University of Southampton; Highfield Southampton SO17 1BJ, UK; United Kingdom
[b] Centre for Electronics Frontiers, Zepler Institute for Photonics and Nanoelectronics, University of Southampton; Highfield Southampton SO17 1BJ, UK; United Kingdom

ARTICLE INFO

Keywords:
Aluminium
Battery
Ionic liquid
Poly(3,4-ethylenedioxythiophene) (PEDOT)
Rechargeable/secondary
Sustainable

ABSTRACT

Research on aluminium batteries is rapidly gaining momentum as a potential alternative to established battery chemistries such as lithium ion. Aluminium is abundant, recyclable, and due to its three-electron redox reaction it offers the potential for high specific energy and power. It can also be used as a metal negative electrode due to its dendrite-free plating behaviour at relevant conditions in room temperature ionic liquid electrolytes. With these electrolytes, a battery made entirely of abundant elements can also be envisaged. However, in order to commercialise aluminium batteries, researchers must still overcome formidable challenges, because no positive electrode material has yet demonstrated efficient reversible storage of aluminium ions. This review paper provides a critical summary of the research to date. We present a discussion of the chemistry of the electrolytes, the deposition and dissolution behaviour of aluminium, and the various cathode materials that have been attempted. We also place non-aqueous aluminium batteries in context with other battery systems and provide an outlook of future research direction, and potential future applications. Using clear graphics to explain the various concepts, we intend this review to provide a broad and clear introduction to the field for researchers new to the area.

1. Introduction

In the effort to move away from fossil fuels, humanity urgently needs affordable, sustainable, long cycle life and high-performance energy storage. The integration of large percentages of intermittent renewable energy sources into electrical grids requires large scale storage to balance supply and demand [2]. Meanwhile, electric vehicles are creating demand for extremely high specific energy batteries to facilitate ranges comparable to current petrol and diesel vehicles (at least 320 km for about 50% of consumers to consider the range acceptable [3]). These must also become more affordable, as approximately half of the current electric vehicle cost is the battery pack [4]. To date, only nations that heavily subsidise their purchase (i.e. Norway) have achieved widespread uptake of electric vehicles [5]. It has been estimated that for electric cars to become price competitive in 50% of the US market, battery pack cost would have to fall from around $230/kWh in 2017 to $150/kWh [3].

Lithium-ion batteries currently dominate for new-build grid storage, electric vehicles, and electronic devices due to their outstanding specific energy and acceptable specific power. This position is reinforced by economies of scale and technological maturity resulting from nearly four decades of development for electronic devices and more recently for electric vehicles [6]. A common fear is that lithium supplies will soon run out; this fear is misplaced as mineral deposits are plentiful. However, price is rising because demand is outstripping supply from the cheaper brine extraction methods. These brines are typically found in the Andes (Chile, Bolivia) and the USA, and provide around half of the world's lithium, with increasing proportions coming from more expensive mineral deposits. Because this is making mineral deposits economic to mine, a lithium mining boom may subsequently drive down price [7].

Another major issue with lithium-ion batteries is the use of cobalt and nickel in the commonly used lithium-cobalt-oxide ($LiCoO_2$), nickel-manganese-cobalt (NMC) and nickel-cobalt-aluminium (NCA) positive electrodes. Lithium-ion batteries consume over 50% of the world's primary cobalt production, of which around 66% is mined in the Democratic Republic of the Congo. There is a well-reported history of human rights abuses in the nation, including widespread use of child labour [8]. Additionally, despite the fact that lithium-ion batteries contain valuable quantities of cobalt, nickel, lithium, iron, copper and aluminium, and that failure to recycle them can lead to environmental damage due to leaching of the toxic components, the difficulty of extracting these elements is so great that significant research effort is still required to make recycling economically viable [9]. It is likely that improvements in

* Corresponding author.
** Corresponding author.
E-mail addresses: bc1g08@soton.ac.uk (B. Craig), capla@soton.ac.uk (C. Ponce de Leon).

https://doi.org/10.1016/j.rser.2020.110100
Received 25 February 2020; Received in revised form 10 July 2020; Accepted 14 July 2020
Available online 1 August 2020

Symbols and abbreviations

[BP]Cl	Butylpyridinium chloride
[EMIm]Cl	1-ethyl-3-methylimidazolium chloride
6-31G*	Pople's split valence double-ζ basis set with polarization functions
AIMD	*Ab initio* molecular dynamics
Al	Aluminium
$Al_2Cl_7^-$	Heptachlorodialuminate
Al^{3+}	Trivalent aluminium ion
$AlCl_3$	Aluminium chloride
$AlCl_4^-$	Tetrachloroaluminate
B3LYP	Becke's hybrid 3-parameter DFT functional [1]
C	C rate – the rate of discharge that discharges the capacity of the battery in 1 h
Ca	Calcium
Cl	Chlorine anion
Cl_2	Chlorine
COP	Conducting organic polymer
DES	Deep eutectic solvent
DFT	Density functional theory
DMSO	Dimethylsulfone
EDOT	3,4-ethylenedioxythiophene
$EMIm^+$	1-ethyl-3-methylimidazolium cation
EQCM	Electrochemical quartz crystal microbalance
HCl	Hydrochloric acid
IL	Ionic liquid
LED	Light emitting diode
$LiCoO_2$	Lithium cobalt oxide
Li-ion	Lithium ion
MDNO	Modified neglect of diatomic overlap
MEIC/EMIC	Pseudonyms of [EMIm]Cl
Mg	Magnesium
Na	Sodium
PEDOT	Poly(3,4-ethylenedioxythiophene)
PPy	Polypyrrole
PTFE	Polytetrafluoroethylene
PVDF	Polyvinylidene fluoride
RTIL	Room temperature ionic liquid
RVC	Reticulated vitreous carbon
SHE	Standard hydrogen electrode
XAS	X-ray absorption spectroscopy
XRD	X-ray powder diffraction
Zn	Zinc
ε	Dielectric constant

recycling technology combined with rises in the price of the constituent elements of lithium-ion batteries will eventually cause recycling to become economically viable, however, and recycling might then provide a substantial proportion of the raw materials for new lithium-ion batteries.

Fire risk is another major issue with lithium-ion batteries. There is inherent flammability associated with lithium-ion and the organic solvents in the electrolyte [10,11]. If the batteries experience an internal short circuit due to damage or dendrite formation, or are heated past a critical temperature, they may undergo exothermic breakdown, termed thermal runaway. This is a violent thermal event that often results in the destruction of the entire battery pack and associated device or vehicle [12]. This problem can be even worse for large scale recycling of lithium batteries where large quantities of cells are stored in one place and purposefully dismantled: a thermal runaway of a single cell can then trigger the destruction of the entire store [9].

All these reasons motivate research into other battery chemistries: even if alternatives cannot match lithium-ion on performance, perhaps they can offer cheaper, safer, more environmentally friendly and ethical options for applications such as grid storage. Aluminium is an attractive metal for a battery system for several reasons. It is low density, affordable, and is the most abundant metal in the Earth's crust [13]. It forms a trivalent cation (Al^{3+} or Al(III)), releasing three electrons per ion relative to monovalent lithium's single electron [14]. As a result, aluminium has a specific energy of 3.0 Ah g^{-1}, slightly lower than lithium metal at 3.9 Ah g^{-1}, and also has an energy density of 8.0 Ah cm^{-3} [13], higher than lithium metal at 2.06 Ah cm^{-3} [15]. Additionally, aluminium can be repetitively stripped and deposited without forming dendrites that might cause short circuits [16], unlike lithium metal [17,18]. The currently used electrolytes in aluminium batteries - room temperature ionic liquids (RTILs) – are non-flammable [19], and there is no need for rare elements. There would be a strong economic case for recycling: recycled aluminium requires only 5% of the energy needed for primary production [20], and disassembly would be straightforward due to the non-flammable electrolyte and a plain aluminium electrode that could be relatively easily removed.

Aluminium batteries naturally find themselves compared to other lithium-ion alternatives such as alkali-ion (sodium and calcium), and multivalent metal batteries (magnesium, zinc). Sodium-ion batteries currently attract the most research attention of any lithium alternative battery due to the similarity to lithium-ion battery operation and the abundance of sodium. However, the larger size of the sodium ion causes poor cycle life, rate capability, and specific energy/energy density. Sodium is also a reactive metal, and the electrolytes are generally organic, so are also flammable. The specific energy is worsened by the inferior potential of $Na|Na^+$ compared to $Li|Li^+$. The reversible and durable storage of sodium ions in the negative electrode is a major hurdle as sodium does not intercalate properly into graphite [21]. A prototype 18650 (18 mm diameter, 65 mm length – standard lithium-ion cell size) cylindrical sodium-ion cell has been demonstrated with an energy density of 90 Wh kg^{-1} compared to commercial lithium-ion at 200–250 Wh kg^{-1} [22,23].

Beyond sodium-ion, calcium batteries are in their infancy. The current generation of electrolytes cause a solid electrolyte interphase (SEI) layer to form on the surface of the calcium negative electrode. This causes very slow calcium deposition and dissolution. Additionally, little progress has been made on positive electrode selection [24]. Zinc secondary batteries use a metallic zinc negative electrode, but despite great research effort still suffer from dendrite formation – a problem that can be avoided in batteries with a flowing electrolyte [25–29]. Finally, magnesium plates without dendrite formation, but the magnesium negative electrode causes extremely high internal resistance. No electrolyte with a full range of suitable properties has been found, and reversible positive electrode materials have yet to be identified [30]. As will be discussed, batteries with an aluminium negative electrode have been demonstrated that do not suffer from any of these issues.

This review is necessarily limited to non-aqueous aluminium batteries; however, it is worth mentioning research taking place on aluminium batteries outside this remit. Aluminium batteries with aqueous electrolytes are being explored (benefits include very high ionic conductivity and non-corrosive, non-toxic electrolytes). Conventional aqueous electrolytes where water is the solvent are not competitive on specific energy, partly because the deposition of aluminium occurs at a more negative potential than the evolution of hydrogen [31] (−1.76 V *vs.* standard hydrogen electrode (SHE) [32]), so an anodic intercalation reaction at a less negative potential must be used [33]. These aqueous systems perform more like supercapacitors, demonstrating specific energy of 15 Wh kg^{-1} and specific power of 300 W kg^{-1} based on positive

and negative electrode masses [15].

A more promising system has recently been reported using super-saturated solutions of $AlCl_3$ in water to allow deposition of Al^{3+} onto an aluminium negative electrode with a graphite positive electrode storing chloroaluminate species. The super-saturation of the electrolyte prevents the evolution of hydrogen and provides an operation and performance similar to aluminium-graphite batteries (see Section 5.1.1), while addressing the cost issue of ionic liquid electrolytes [34]. Similarly work continues on metal-air batteries including aluminium-air [35]. Metal-air batteries can be characterised by offering very good performance as a primary battery and theoretical specific energy and energy density that exceeds any existing secondary battery. However, all metal-air batteries face the same serious issues in recharging (including irreversible consumption of the electrodes), and so currently cannot be described as being rechargeable [36].

2. Mode of operation of non-aqueous aluminium batteries

The most promising aluminium batteries work on a different principle to lithium-ion batteries. Lithium-ion batteries operate according to the well-known rocking-chair mechanism where lithium ions travel from the negative to the positive electrode as the battery is discharged [37] with the electrolyte acting only as a transport media. Ideally, aluminium batteries would work in a similar way because this would require minimal quantities of electrolyte. The positive electrode would largely determine the specific energy and energy density of the battery. However, attempts to store aluminium ions in a positive electrode have at best demonstrated unacceptably low discharge potential, capacity, coulombic efficiency and cycle life (see section 'Proposed positive electrodes storing Al(III)'). This is due to the trivalency of the aluminium ion, causing aluminium to have a strong charge interaction with the host material, and preventing reversible charge storage [38–41].

The main approach taken to avoid this problem is to store monovalent $AlCl_4^-$ and $Al_2Cl_7^-$ anions from the RTIL electrolyte in the positive electrode instead of Al(III). At partial charge a mix of species is stored, but as the battery is fully charged the $Al_2Cl_7^-$ is depleted, so only $AlCl_4^-$ is stored [13,42]. This leads to a fundamental difference in battery operation compared to lithium-ion batteries because these species are stored in the positive electrode during charge, not discharge [13]. Therefore, when aluminium batteries are charged, $Al_2Cl_7^-$ species in the electrolyte are split into aluminium ions, which are deposited, and $AlCl_4^-$, which is stored at the positive electrode. The full-cell equation is shown by Equation (1) [43]:

$$4Al_2Cl_7^- + Cathode_x \rightleftharpoons Cathode_x\left[7AlCl_4^-\right] + Al \qquad \text{Equation 1}$$

The mechanism of a battery with an aluminium negative electrode, graphite positive electrode and a Lewis acidic $AlCl_3$-[EMIm]Cl electrolyte is shown in Fig. 1. In the ratios used in aluminium batteries, the $AlCl_3$ and [EMIm]Cl complex to form a solution containing $[EMIm]^+$ cations and a combination of $AlCl_4^-$ and $Al_2Cl_7^-$ anions.

Because both electrodes in the aluminium battery store species during charge and release them during discharge, the electrolyte must hold all the electroactive species when the cell is fully discharged. Because the electrolyte can only support a certain range of composition, the specific energy and energy density of the battery are dependent on the amount of electrolyte [42], unlike rocking-chair batteries where only enough electrolyte is required to saturate the electrodes. This has led some researchers to suggest that the electrolyte is actually the negative electrode and the batteries should be named aluminium-chloride batteries [42]. However, we simply refer to these systems as aluminium batteries [45]. The dependence on the quantity of electrolyte means that some authors have started to calculate energy density of aluminium batteries using the following formula. F is Faraday constant (26.8×10^3 mAh mol^{-1}), x is the number of electrons involved in reducing 1 mol of $AlCl_3$ (0.75), r is the maximum molar ratio of the electrolyte (2), Q_C is the specific capacity of the positive electrode (in mAh g^{-1}), and $M(AlCl_3)$ and $M(EMImCl)$ are the molar masses of $AlCl_3$ and EMImCl (133.34 g mol^{-1} and 146.62 g mol^{-1} respectively) [42].

$$Q_{spec} = \frac{Fx(r-1)Q_c}{Fx(r-1) + Q_c(rM(AlCl_3) + M(EMImCl))} \qquad \text{Equation 2}$$

This accounts for the entire volume of electrolyte required and the mass of active positive electrode in the discharged state (it is assumed that the fully discharged battery will have no active aluminium at the negative electrode at all). This limits the specific capacity of aluminium batteries to 48.6 mAh g^{-1} (in the limit of a positive electrode with infinite specific capacity) [13]. Using the highest value yet reported of 192 mAh g^{-1}, for a PEDOT positive electrode, gives a full battery capacity of 39 mAh g^{-1} [46].

3. Electrolytes for non-aqueous aluminium batteries

Over the history of aluminium electrochemical deposition, electrolyte research focus has progressed from organic solvents [47] to room temperature ionic liquids (RTILs). Even within these categories, the choice of electrolytes that are able to reversibly deposit aluminium over a useful electrochemical range is extremely limited [48]. RTILs are a significant improvement over organic solvents [49], which are volatile, flammable and only allow low current densities [33,50], and to our knowledge organic electrolytes have never been used in aluminium battery research.

A suitable electrolyte for aluminium deposition must fulfil a number of criteria. The solute must be highly soluble in the solvent, but should not be held in solution so strongly that aluminium cannot be deposited. Reversible aluminium deposition/dissolution must occur within the electrochemical potential window bound by the limits at which electrolyte decomposition, electrode reaction with solvent, or other undesirable reactions occur. Finally, the electrolyte must have low viscosity at operating temperatures, in order to provide high ionic conductivity and mobility, so that the electrolyte does not contribute with a high resistance to the battery. It must also plate the aluminium negative electrode reversibly without dendrite formation [33,51].

It is worth clarifying the differences between ionic liquids, molten salts, and deep eutectic solvents. Ionic liquids are liquid salts, consisting exclusively of weakly coordinated complex ions that are liquid below 100 °C or at room temperature. Molten salts are liquefied salts at high temperatures (~800 °C) and deep eutectic solvents are mixtures with a melting point much lower than their anionic and cationic components have on their own. The type of ionic liquids that are liquid at room temperature are called RTILs, and as batteries typically operate relatively near to this temperature, these are suitable candidates for battery electrolytes [19]. In fact, it is loosely conventional to describe any molten salt that is liquid below 100 °C as a RTIL, but it is important to recognise that this distinction is arbitrary [52].

3.1. Room temperature ionic liquids (RTILs)

The start of modern research on room temperature ionic liquids (RTILs) suitable for aluminium batteries began in the early 1970s, and by 1990, three RTILs had emerged: $AlCl_3$-1-butylpyridinium chloride ($AlCl_3$-[BP]Cl) [19,53–55], trimethylphenylammonium chloride ($AlCl_3$-TMPAC) [56,57], and 1-methyl-3-methylimidazolium chloride ([EMIm]Cl) (synonymous with 1-ethyl-3-methylimidazolium chloride [56–60], and also known as EtMeImCl, MeEtImCl, MEIC and EMIC [58,61]). Of these, [EMIm]Cl has the widest electrochemical window (0.8 V lower reduction potential than [BP]Cl), best liquidus temperatures and aluminium reactivity, while maintaining the conductivity, viscosity, Lewis acidity range, and solvation ability of the other salts. This has led to its almost exclusive use in current non-aqueous aluminium battery research [56–58,62]. Relative to organic solvents, RTILs have good ionic conductivity, good thermal stability, low vapour pressure, and a wide

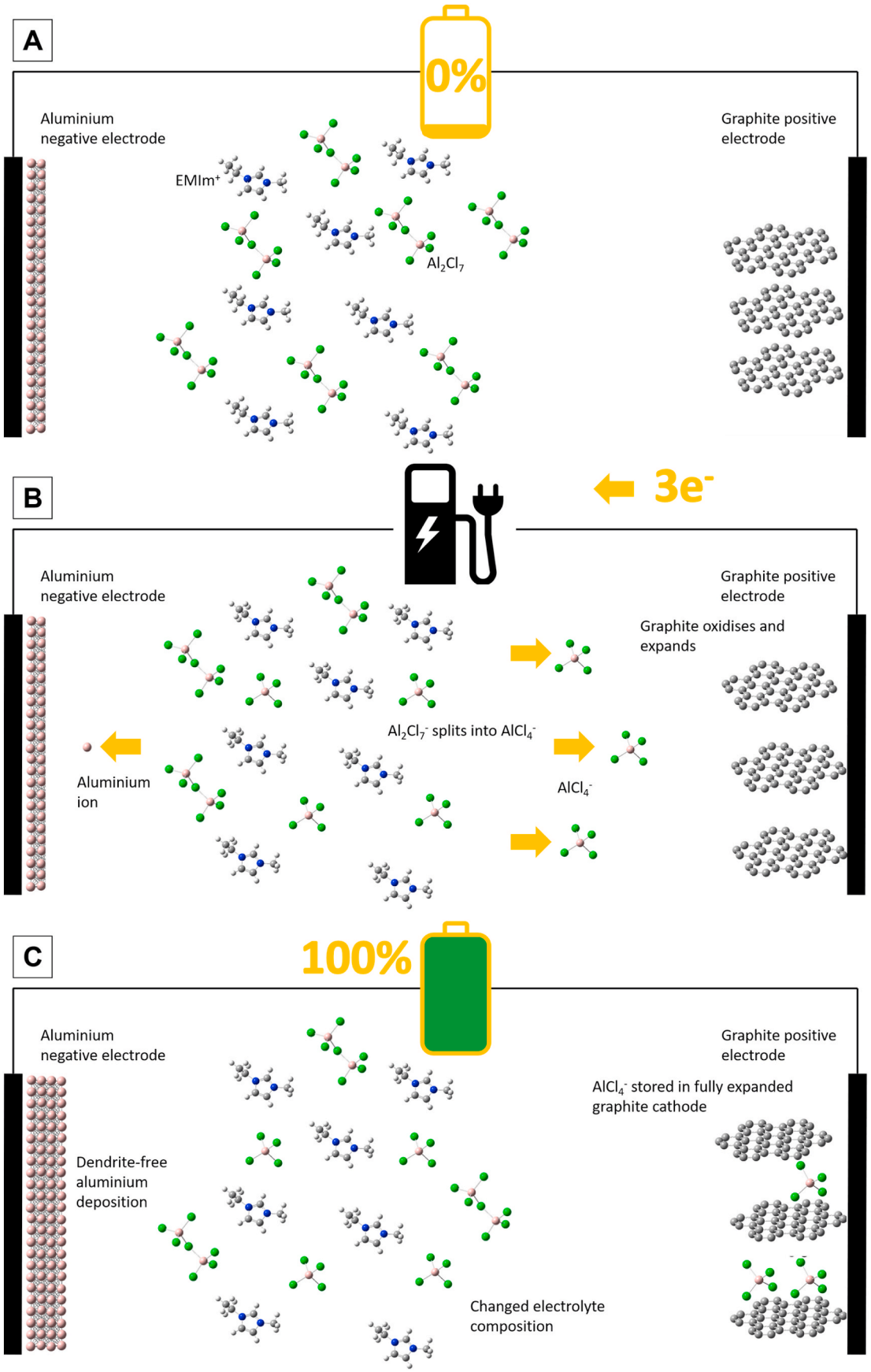

Fig. 1. Charging of a battery with aluminium negative electrode, graphite positive electrode and $AlCl_3$-[EMIm]Cl electrolyte showing A) fully discharged, B) charging, C) fully charged (molecules drawn using Gaussview/Gaussian [44]).

electrochemical potential window [56], and can sustain much higher rates of deposition [33]. To date, applications for RTILs have included fuel cells, electrochemical capacitors, solar cells, lithium-ion and lead acid batteries, and electrolytes in sensors [63].

While tailoring of RTILs with various additives has been attempted for purposes such as reduced moisture sensitivity, these have not yet been explored in aluminium batteries. Extra additives would lower the specific energy, and it makes sense to avoid moisture completely through experimentation in inert environments [64]. Difficulties with $AlCl_3$-[EMIm]Cl are mainly in its preparation, which must be done in an inert atmosphere due to the hygroscopicity of $AlCl_3$, and slowly due to the exothermic nature of the mixing process. $AlCl_3$ is low cost and widely available, but [EMIm]Cl is still a relatively niche component with a small supply chain, although it is made of abundant elements and large-scale manufacturing could probably make it economical. It is also hard to purify, and there is a lack of detailed information on its toxicity due to its use not yet having become widespread [60,62,63]. Chloroaluminate Lewis acidic RTILs are highly corrosive, and $AlCl_3$ reacts violently with water and is a severe irritant [49]; however these difficulties are mitigated by handling in a glovebox.

For optimal battery performance, moisture content should be as low as possible, again implying use of a glovebox. Even a low level of moisture significantly impairs coulombic efficiency due to HCl and Cl_2 evolution [43]. As more water is added, the ionic nature of the mixture is reduced because large hydrogen-bonded clusters and networks formed of water molecules begin to form, separating the ions from each other and significantly altering the chemistry [65]. Water reduces the electrochemical potential window of RTILs; for example, from 4.10 V to 1.95 V in [BMIM][BF4] when 3 wt% water is added. Finally, water can also react with ILs to create different electroactive species [66].

RTILs have a wide liquidus range that goes down to around −80 °C [63], and $AlCl_3$-[EMIm]Cl is thermally stable to +95 °C; above which highly coloured decomposition products form [33,67,68]. While this wide temperature range seems appealing for batteries, the viscosity and hence ionic conductivity of RTILs is strongly dependent on temperature [69]. At room temperature, a typical aqueous lead acid electrolyte conductivity is around 730 mS cm^{-1}, while ionic liquids and lithium-ion electrolytes have conductivities in the region of 10–20 mS cm^{-1} [19]. It is possible to enhance the conductivity and reduce the viscosity of these melts without changing the types of species formed by adding organic solvent [55,70], however this would reduce the 'greenness' of the mixture. Over the full liquidus range, RTILs have very low vapour pressure. This provides low volatility and is a major reason why ionic liquids are considered 'green solvents'. This is attributable to high cohesive energy density, caused mainly by strong Coulombic interactions between the components of the ionic liquids [71].

3.1.1. *$AlCl_3$-[EMIm]Cl chemistry*

The speciation behaviour of $AlCl_3$-[EMIm]Cl is largely responsible for the operation of the aluminium battery [49], so warrants detailed discussion. While [EMIm]Cl will always dissociate to $[EMIm]^+$, the type of chloroaluminate species formed, and the Lewis acidity, depends on the molar ratio of $AlCl_3$ to [EMIm]Cl. The parameter r is the molar ratio of $AlCl_3$ to [EMIm]Cl. For example, $r = 2$ means 2 mol of $AlCl_3$ to 1 mol

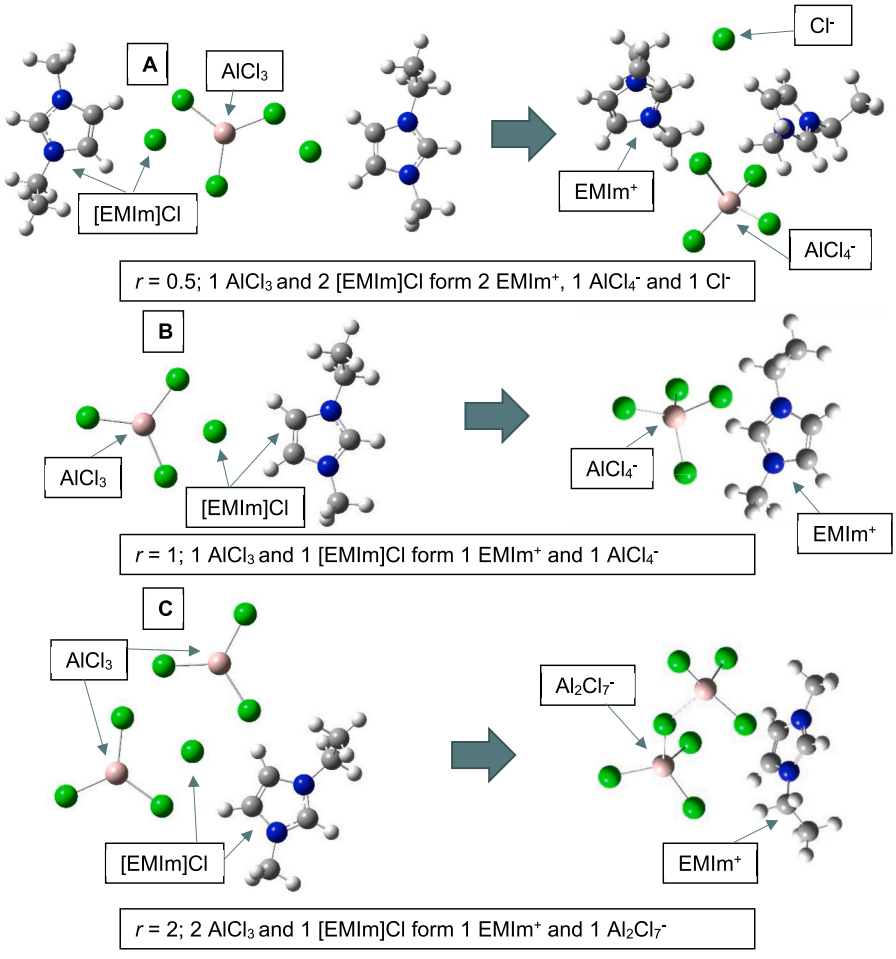

Fig. 2. *Formation of chloroaluminate species at different r values of $AlCl_3$-[EMIm]Cl (molecule drawn using Gaussview/Gaussian [44]).*

of [EMIm]Cl. The effect of r on speciation is shown in Fig. 2. If $r < 1$, a Lewis basic electrolyte containing $AlCl_4^-$ and Cl^- is produced. $r = 0.5$ is shown in *(a)*. If $r = 1$, a neutral mix results; this will contain only $AlCl_4^-$. $r = 1$ is shown in *(b)*. The deposition of aluminium is only possible from $r > 1.1$ liquids [72], where a large proportion of $Al_2Cl_7^-$ is present. The saturation limit of $AlCl_3$ in [EMIm]Cl occurs at $r = 2$ and is shown in *(c)* [38].

As discussed, in the best performing aluminium batteries, chloroaluminate species are stored in the positive electrode during charge [42]. This causes r to increase as the battery is discharged, reaching a maximum when the battery is fully discharged and a minimum when the battery is fully charged. It is only possible to deposit aluminium for r values between 1.1 and 2 [42,72]. This influences the chloroaluminate ions available to store in the positive electrode. At $r = 1.1$, the battery is fully charged and $Al_2Cl_7^-$ is depleted, so only $AlCl_4^-$ is stored [42] while at partial charge levels both are present [13].

The balance of species present is driven by Equations (3)–(5). K is equilibrium constant and the given values are specific to $AlCl_3$-[EMIm]Cl at 40 °C [73].

$$Cl^-(l) + AlCl_3(s) \rightleftharpoons AlCl_4^-(l), \quad K = 1.6 \times 10^{19} \qquad \text{Equation 3}$$

$$AlCl_4^-(l) + AlCl_3(s) \rightleftharpoons Al_2Cl_7^-, \quad K = 1.6 \times 10^{3} \qquad \text{Equation 4}$$

$$Al_2Cl_7^-(l) + AlCl_3(s) \rightleftharpoons Al_3Cl_{10}^-(l), \quad K = 1.0 \times 10^{1} \qquad \text{Equation 5}$$

The very high equilibrium constant of Equation (3) shows that when Cl^- and $AlCl_3$ are mixed in equal proportions, the result will be the overwhelming formation of $AlCl_4^-$. The intermediate equilibrium constant of Equation (4) shows that when $AlCl_4^-$ is combined with additional $AlCl_3$, a mixture of $AlCl_4^-$ and $Al_2Cl_7^-$ is formed. Finally the low equilibrium constant of equation (5) shows that when further $AlCl_3$ is added to a solution already rich in $Al_2Cl_7^-$, there is a low tendency for $Al_3Cl_{10}^-$ to form [74]. These equations combine to give Lewis acid/base behaviour for $AlCl_3$-[EMIm]Cl that depends on the concentration of $AlCl_3$ to [EMIm]Cl, whereby two amphoteric, uncharged solvent molecules undergo a Lewis acid transfer, as shown in Equation (6) [73].

$$AlCl_4^-(l) + AlCl_4^-(l) \rightleftharpoons Al_2Cl_7^-(l) + Cl^-(l), \; K = 10^{-16} \qquad \text{Equation 6}$$

In a Lewis neutral $AlCl_3$-[EMIm]Cl liquid, the electrochemical limits are due to $EMIm^+$ being reduced and $AlCl_4^-$ being oxidised. This gives the widest electrochemical window – from around −2 V to +2.7 V *vs.* Al|Al(III), providing the electrolyte is free of moisture. For a Lewis acidic liquid however, $Al_2Cl_7^-$ reduces at 0 V to deposit aluminium on the electrode. In Lewis basic liquids, $EMIm^+$ becomes the cathodic limit as $Al_2Cl_7^-$ is not present, but the presence of Cl^- means that Cl^- evolves before $AlCl_4^-$, reducing the anodic limit to about −1 V *vs.* Al|Al(III) [73]. Because $EMIm^+$ is reduced before $AlCl_4^-$, aluminium cannot be deposited from $AlCl_4^-$ within the electrolytic limits of the electrolyte, which is why only acidic electrolytes can be used for aluminium deposition/dissolution [67]. Above the discharge potential window of the electrolyte, side reactions involving Cl_2 evolution from the electrolyte begin to occur, particularly above 2.6 V *vs.* Al|Al(III) [43,75]. A graph showing the electrochemical potential range of basic, neutral and acidic $AlCl_3$-[EMIm]Cl is shown in Fig. 3 [73].

3.1.2. RTIL gel electrolytes

Extending the electrochemical stability window of the ionic liquid electrolyte to – 2 V *vs.* Al|Al(III) would stabilise the $[EMIm]^+$ sufficiently to allow deposition of aluminium from $AlCl_4^-$. Because the required quantity of electrolyte drives the specific energy and energy density of non-aqueous aluminium batteries storing chloroaluminate species at the positive electrode, this could substantially improve overall battery performance.

One promising way to achieve this is by the addition of a gelification component e.g. a polymer, though the amount must be carefully chosen as it will compromise the ionic conductivity [76–80]. The simplest approach is to introduce a small amount of non-reactive polymer into the ionic liquid, tangling the molecules of the ionic liquid, restricting their movement enough to give the electrolyte rubber-like or gel-like properties. These are referred to as gel electrolyte or ion gels, and suitable polymers include poly(phenylene oxide) (PPO), poly(methyl methacrylate) and poly(vinylidene fluoride) [77,81]. However, these mixtures can experience problems such as phase separations, where some of the ionic liquid becomes separated from the polymer, which can lead to leakage [77]. It has been shown that simply by adding 10 wt-% PEO to an $r = 1$ $AlCl_3$-[EMIm]Cl electrolyte, the potential stability window of the electrolyte can be increased by 1 V, but the coulombic efficiency of aluminium deposition/dissolution is brought down to below 60% [82].

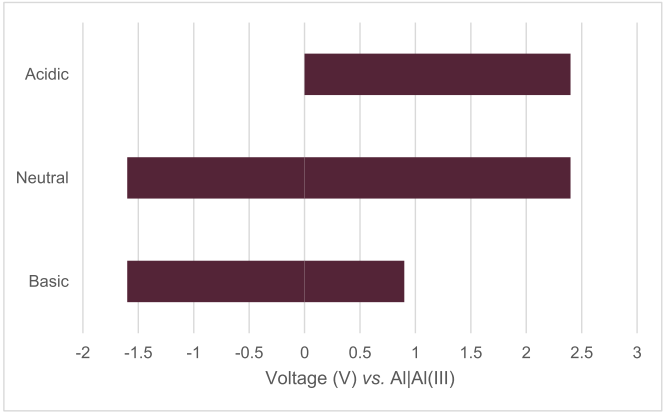

Fig. 3. *Electrochemical potential range of $AlCl_3$-[EMIm]Cl at Lewis basic (r = 0.89), neutral (r = 1.0) and acidic (r = 1.2) compositions (adapted from Ref. [73]).*

Alternatively, it is possible to polymerize a component of the ionic liquid itself, for example the imidazolium cation, which would produce a polymeric ionic liquid (PIL). These also have low ionic conductivity ($<10^{-6}$ S cm^{-1}) relative to ILs (10^{-2} S cm^{-1}), raising the possibility of further tailoring by combining PILs with RTILs to gain a further intermediate compromise in electrolyte characteristics (10^{-3} to 10^{-5} S cm^{-1}). Due to being molecularly close to ILs in the first instance, PILs mix better with ILs than polymers, potentially helping to avoid some of the aforementioned weaknesses with polymer/IL combinations [77].

3.2. Deep eutectic solvents

A Deep Eutectic Solvent (DES) is a mixture of at least two components, which independently might be solids or liquids at room temperature, that when combined in a particular (eutectic) range of composition have a melting point up to 200 °C lower than either constituent on its own [63,83,84]. Similar to ionic liquids, they contain a combination of Lewis or Brønsted-Lowry acids and bases that when solvated in one another form a range of species that may be anionic and/or cationic [85]. DESs are made of readily available, abundant, cheap materials, and are synthesized through simple mixing of the components [86], generating only moderate heat [83]. By intent, many DESs are more environmentally friendly than ILs, as in addition to having low vapour pressure, they commonly contain no components of known or unknown toxicity [63,84]. Indeed, there is a subclass of DESs which are particularly benign, termed natural deep eutectic solvents (NADES), which consist only of bioavailable complexing agents such as choline, amino acids or their metabolites such as urea or sugars [84]. It may be that DESs are entering a period of rapid growth in research interest, as for ionic liquids in the 1990s [84]. DESs have already been used in a range of applications including electropolishing, synthesis of gold nanoparticles, metal oxide processing and biodiesel purification

[63].

DESs are little researched for aluminium deposition [83] despite the work of a few key authors [87] but initial research is somewhat encouraging, with aluminium deposition demonstrated from DESs including $AlCl_3$-4-propylpyriinde (4-Pr-Py) [88], $AlCl_3$-acetamide [89], and $AlCl_3$-urea with 1,2-dichloroethane [90]. The lack of $Al_2Cl_7^-$ means that $AlCl_3$-4-Pr-Py is less water sensitive than $AlCl_3$-[EMIm]Cl [88]. DESs have reduced electrochemical redox potential window relative to RTILs [63,91] and poor ionic conductivity. Organic solvents could improve this but would make DESs less environmentally friendly [85, 90]. The composition range for aluminium deposition is also less ($r = 1.1$ to 1.5 for $AlCl_3$-acetamide) than for $AlCl_3$-[EMIm]Cl [89]. While DESs are generally less affected by moisture than chloroaluminate ionic liquids [63], these benefits are limited for those DESs containing $AlCl_3$, which to date is all those from which aluminium has been deposited [87]. While worse performing than RTILs at the moment, it is possible that DESs may see developments in the future that increase their appeal.

4. Aluminium deposition and dissolution

One of the key benefits of aluminium is its dendrite-free behaviour when deposited/dissolved at moderate current densities onto a suitable substrate such as aluminium, tungsten or planar vitreous carbon in chloroaluminate RTILs, a behaviour which it shares with magnesium [92]. The use of plain metal anodes is highly preferable to storing the active ions in a host negative electrode due to savings in mass, complexity and volume. Many metals used in batteries, including sodium, zinc and lithium, tend to form dendrites when the metal is repeatedly stripped and plated during charging [17,28,93], which has for example prevented the development of safe lithium metal batteries [17].

When aluminium is deposited from $AlCl_3$-[EMIm]Cl, dendrites only form above current densities of 100 mA cm^{-2} [56]. This is due to plating occurring faster than diffusion can supply species from the electrolyte, causing preferential plating onto protruding parts of the electrode, leading to dendrite growth [27,94]. Fortunately, current densities are much lower than this in batteries (80 C can be achieved at 10 mA cm^{-2}) [95]. An Al–Ni_3S_2 battery with a $LiAlCl_4$–$NaAlCl_4$–$NaAlBr_4$–$KAlCl_4$ non-organic electrolyte functioned without dendrites at 70 mA cm^{-2} and below, and still without dendrites but with a slightly less dense plating from 100 to 706 mA cm^{-2} [96]. When electrodepositing aluminium from $r = 2$ $AlCl_3$-[EMIm]Cl, dense plating has been achieved up to 70 mAh g^{-1} [56,72]. Clearly, the choice of electrolyte is critical in obtaining a dendrite-free plating behaviour.

Aluminium negative electrodes in chloroaluminate electrolytes do not form a solid electrolyte interphase layer (a layer that forms on the electrode surface and separates it from the electrolyte) [97], so deposition and dissolution occur at the electrolyte/aluminium interface. Aluminium diffusion energy is less than 1/3 of that predicted by conventional diffusion mechanisms. This is due to an exchange-diffusion mechanism, where an aluminium atom with metallic bonding on the surface is extracted in exchange for another aluminium atom becoming covalently bonded [98–100]. This mechanism is the only exception known to the hard-sphere model of diffusion where an adatom will follow the lowest-energy diffusion route along a surface channel, and applies only to the (001) surfaces of platinum, nickel, aluminium and iridium [99]. Aluminium self-diffusion energy at 0.17 eV is nevertheless higher than either magnesium at 0.02 eV, which reliably plates without dendrite formation [101], or 0.14 eV for lithium and 0.16 eV for sodium, which do not [102]. However, the real benefit of the exchange-diffusion mechanism is that it has been shown in simulations to cause aluminium atoms to move down from protrusions and spread out across the plating surface in even layers, regardless of the diffusion energy [100].

Aluminium crystal structure is face-centred cubic (fcc) [92], which has a high coordination number of 12 [103], also supporting the development of a stable crystal structure through increased lattice stability. This is like magnesium, which also has a co-ordination number of 12 due to its hexagonal close packed (hcp) structure. In contrast, lithium and sodium are both body-centred cubic (bcc) with a lower co-ordination number of eight [93,104]. The mechanism is that higher co-ordination number metals have a higher driving force to re-organise into high-coordination configurations, which tend to be achieved better by a dense, even layer rather than through dendrite formation [105].

Most papers reporting on aluminium deposition from ionic liquids found that instantaneous nucleation occurred (from $AlCl_3$-BMIC, $AlCl_3$-[EMIm]Cl [56,106] and $AlCl_3$-TMPAC [67]), with only one paper reporting progressive nucleation (also from $AlCl_3$-[EMIm]Cl) [107]. When plated from ionic liquids, aluminium follows a hemispherical (3D) growth process, which means that as the initial nuclei grow on the surface, the electroactive species are drawn from the electrolyte, creating a diffusion zone with a deficiency of electroactive species in the electrolyte. The diffusion zone grows ahead of the hemispherical nuclei into the electrolyte (hence 3D growth), and creates a 'shadow' region of electroactive species depletion on the electrode face, creating an exclusion zone where nucleation can no longer take place so that new nucleation is forced to take place elsewhere [107]. The hemispherical nuclei grow by diffusion until they meet. At this point, they coalesce into a layer (going from a 3D growth mechanism to a 2D planar growth mechanism) [67].

Once a crystal structure is established in the layer, further growth of the layer may be limited by either diffusion or kinetic rates, whichever is slowest [108]. At all but the lowest current densities [97], aluminium layer growth is diffusion limited [67,97,107]. Aluminium can be deposited either directly onto a suitable substrate such as vitreous carbon or an aluminium seed layer [42]. High coulombic efficiency of stripping and plating have been achieved in both organic and RTIL electrolytes, with >99% achievable in both $AlCl_3$-[EMIm]Cl [109] and some organic solvents [110]. Fig. 4 shows SEM images of aluminium deposits obtained from $r = 2$ $AlCl_3$-[EMIm]Cl at 60 °C for 20 min. The top two images refer to deposition at −0.15 V *vs.* Al|Al(III) and the bottom two images to deposition at −0.30 V *vs.* Al|Al(III): the close up pictures show a dense even packing of aluminium crystallites.

A significant factor when dealing with aluminium is the oxide layer that forms upon exposure to air, which reaches a thickness of around 32 Å after just 10 min of exposure [111]. This is an important consideration for manufacturing aluminium batteries, as the oxide layer is insulating, requires additional processing steps to remove, and requires that oxygen must be excluded during battery assembly to avoid its formation [16, 56]. This oxide does not build up if the aluminium is deposited in an inert atmosphere such as inside a glove box. Researchers have also tried to remove the oxide layer from an aluminium negative electrode before experimentation, which is very difficult outside of an inert atmosphere because of the speed with which aluminium re-oxidises in the presence of any oxygen [56,97]. This is an important issue to bear in mind when analysing or carrying out research into aluminium deposition/dissolution.

The cyclic voltammogram of aluminium deposition is shown in Fig. 5. The C (cathodic) area corresponds to the deposition of aluminium and the A area (anodic) to the dissolution; the subscript 1 refers to deposition and dissolution of nanocrystalline aluminium, while 2 refers to deposition and dissolution of microcrystalline aluminium [112]. Above 0.8 V, passivation of the electrode causes the current density to drop to zero [56].

5. Positive electrode materials for non-aqueous aluminium batteries

Positive electrodes for non-aqueous aluminium batteries can be divided into two categories: those that store chloroaluminate species, which have been shown to have high performance, and those that store aluminium, which have not. However, research continues into positive electrodes that store aluminium because if good performance could be

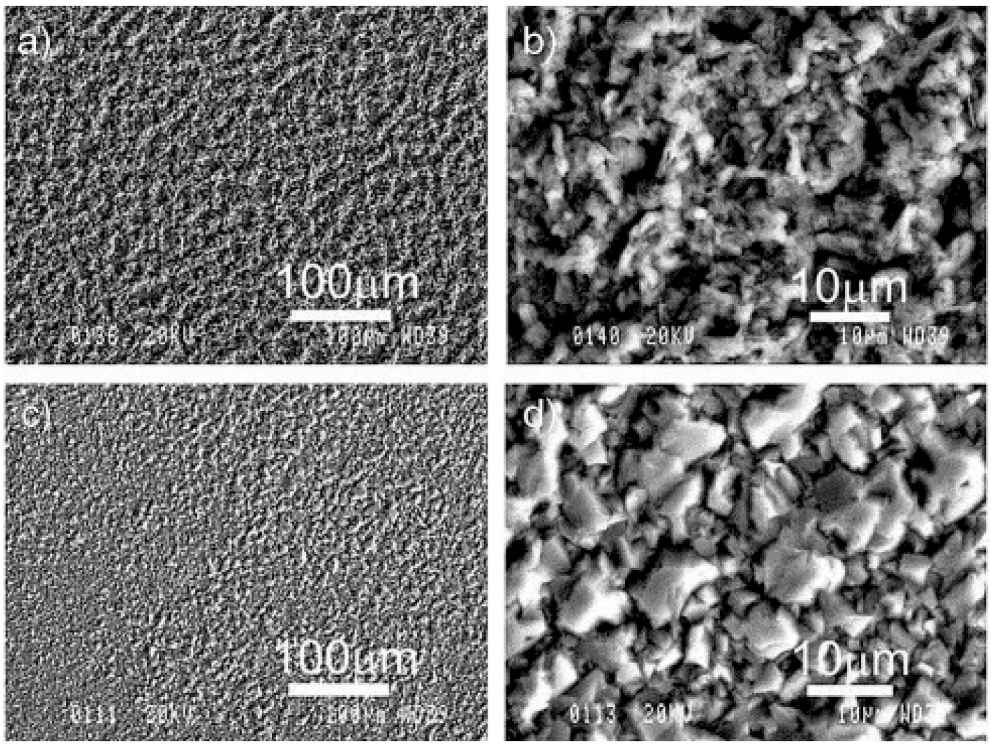

Fig. 4. SEM micrographs of aluminium electrodeposits prepared on Al electrodes from 2:1 M ratio AlCl3–[EMIm]Cl ionic liquids at 60 °C for 20 min. The deposition potentials are −0.15 V (a) and b)) and −0.30 V (c) and d)), respectively. On the right are the higher magnification micrographs displaying more details of the aluminium crystallites. (Reproduced with permission from the Journal of Surface and Coatings Technology [56]).

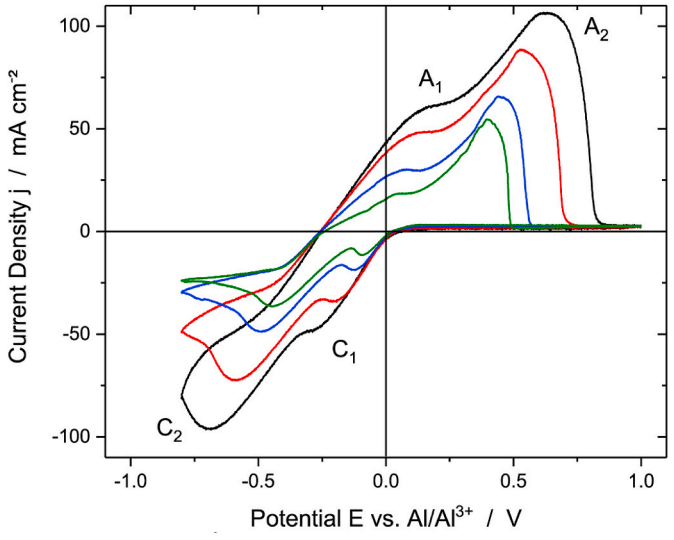

Fig. 5. *Cyclic voltammograms of aluminium deposition on a tungsten electrode in* r *= 2 $AlCl_3$-[EMIm]Cl at sweep rates of* 10 mV s^{-1} *(green),* 20 mV s^{-1} *(blue),* 50 m V s^{-1} *(red) and* 100 mV s^{-1} *(black). (Reproduced under Creative Commons 4.0 [https://creativecommons.org/licenses/by/4.0/] from Refs. [112]).* (For interpretation of the references to colour in this figure legend, the reader is referred to the Web version of this article.)

obtained, the quantity of electrolyte required would be dramatically reduced, as it would no longer have to buffer a compositional change, and so the specific energy of the battery would be greatly increased. Of the materials discussed, graphite, conducting polymers and iron chloride all store chloroaluminate species. Sulphur, vanadium-based positive electrodes, and transition metal sulphides, and anthraquinone electrodes all store aluminium. Proposed positive electrodes that demonstrated no actual storage behaviour in experiments, such as MnO_2, have been omitted [113].

The highest observed specific energy of an aluminium battery with a graphite negative electrode is about 68 Wh kg^{-1}. This takes into account the required quantity of electrolyte mass ($AlCl_3$-[EMIm]Cl, $r = 2$ when fully discharged), as calculated via Equation (2) [114]. Applying the same analysis to PEDOT gives a specific energy of 50 Wh kg^{-1} [46]. In comparison, lithium-ion, based on active components only, can achieve specific energies of over 500 Wh kg^{-1} [10], while commercial lithium-ion cells (including the mass of the battery pouch or case) achieve around 250 Wh kg^{-1} [22]. Fig. 6 demonstrates full cell specific energies *vs.* demonstrated cycle life for some of the discussed positive electrode materials, with lithium-ion included (active materials only) for comparison.

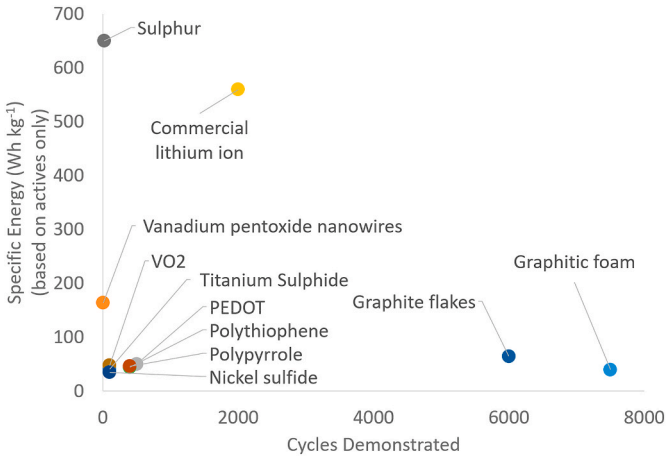

Fig. 6. Specific energies of some research positive electrode materials vs. lithium ion [10,13,40–43,46,115–117].

5.1. Positive electrodes storing chloroaluminate anions

5.1.1. Graphite

The first attempt at a rechargeable aluminium battery with a graphite positive electrode was in 1988 [72]. There were no further publications until 2013 [118], but then took off in earnest from 2015 [43], when Lin et al. produced a battery with a graphitic foam positive electrode that had a cycle life of 7500 cycles, a discharge potential near 2 V *vs.* Al|Al(III), and a coulombic efficiency of 98%. Since then several papers, both experimental and theoretical, have been published investigating various graphite positive electrodes (see Table 1 for the characteristics of many of the reported aluminium-graphite batteries). With a flat discharge potential profile of 1.8–1.9 V *vs.* Al|Al(III) [43,114,119,120], >65 C rate capability, coulombic efficiency > 98% [43], round trip efficiency > 80% [42,114] and achievable specific energy of around 65 Wh kg^{-1} [43,114], aluminium-graphite batteries already compare favourably to lead acid and vanadium redox flow batteries, indicating their potential for large scale grid storage [121]. The cell equation for the Al-graphite battery is shown by Equation (8) [43]:

$$4Al_2Cl_7^- + C_x \rightleftharpoons C_x\left[7AlCl_4^-\right] + Al \qquad \text{Equation 8}$$

Graphite is used ubiquitously in lithium-ion batteries as an intercalation negative electrode [37]. In aluminium batteries, however, it is used as an intercalation positive electrode with an aluminium negative electrode. While aluminium cannot intercalate into graphite, chloroaluminate anions can [122,123]. The charge/discharge of a battery with $r = 1.5$ $AlCl_3$-[EMIm]Cl electrolyte and a pyrolytic graphite positive electrode undergoing galvanostatic cycling at 25 °C is shown in Fig. 7, which shows the initial cycle development (a), very flat discharge potential (a), good life cycle stability (b) and high coulombic efficiency (c) of the aluminium-graphite battery.

While compact lithium ions intercalate easily into round, smooth graphite particles, the much larger chloroaluminate species work far better with a low-defect flaky or foamy morphology (see Table 1). This is because the positive electrode must easily expand to accommodate bulky anion intercalation between the layers of graphite. Pristine (very low defect) graphite flakes allow up to 80% geometric volumetric expansion and fast rates (notably, this is an 80% expansion of the entire positive electrode, which would be difficult to accommodate in a commercialised cell) [42]. Meanwhile, pyrolytic graphite has a very low rate capability and around half the capacity due to covalent bonding between the layers constraining expansion [43]. The high rate capabilities and flat discharge potential profiles observed with graphitic foam [43] and graphite flakes [114] are explained by the fact that all of the possible intercalation positions have very similar and very low energy, so the barrier to $AlCl_4^-$ diffusion in graphite is very low (10 × lower than for lithium) [124]. Graphite has a planar structure, and is described in terms of gallery height, which is the distance (d) between the planar graphite layers (3.34 Å for un-intercalated graphite), and in terms of intercalation stage. This is the period of the repeating sequence of single occupied layers separated by a number of unoccupied layers. Fig. 8 shows a stage 1 single layer intercalation in A, a stage 4 single layer intercalation in B, and a stage 4 double layer intercalation in C.

Researchers have used density functional theory (DFT) and experimental analysis to understand the performance of chloroaluminate intercalation in graphite and to establish the preferred intercalation. One publication suggests that graphite exists in a planar quadrangle structure in graphite [124], but most papers conclude that tetrahedral $AlCl_4^-$ intercalation occurs [120,125,126].

When intercalation occurs, the gallery height of graphite increases. Both modelling and experimentation suggest an increase from a well-defined initial value of ~3.34 Å (all graphite types, experiment and modelling), to values including 5.7 Å (experimental result, pristine graphite foil) [43], 6.025 Å (DFT model, bulk graphite) [124], 8.81 Å [125] (DFT models, bulk graphite), and 8.9–9.3 Å (DFT model, bulk graphite) [122]. These papers all presented DFT modelling results showing that Stage 4 intercalation is the preferred state, although one paper [126] further suggested that Stage 4 would be preferred initially, but as the positive electrode reached full capacity it would shift to Stage 1 intercalation. For bulk graphite, capacities were estimated at ~70 mAh g^{-1} [125,126], close to the theoretically observed values from Ref. [43] for pyrolytic and natural graphite. In contrast, another paper presented strikingly different results, achieved by modelling the graphitic foam from Ref. [43] as a few-layered structure. The diffusion rate was very sensitive to the number of adjacent layers modelled: the rate for 4-layer foam was 48 × faster, and two layers 225 × faster than for bulk graphite. This paper also proposed stage 3 and 4 double stacking even in bulk graphite, with gallery height up to 12.4 Å for bulk graphite and 13.3 Å for graphitic foam, and capacity up to 117 mAh g^{-1} [127]. These results are closer to those obtained for types of graphite flakes (124–142 mAh g^{-1}) [42,114], implying that the DFT modelling approach must fully account for the positive electrode microstructure, because gallery height expansions of this kind cannot be expected to be accommodated by the bulk graphite microstructure.

Table 1
Key performance characteristics of aluminium-graphite battery systems to date.

Positive electrode	Electrolyte	Discharge Potential (V)	Coulombic Efficiency (%)	Cycle Life achieved	C rate achieved	Positive electrode specific capacity (mAh g^{-1})	Specific Energy (Wh kg^{-1})	Reference, year
Graphite powder w. polysulfone binder	$AlCl_3$-DMPrICl r = 1.5	1.7	80–90	195	0.25	35 to 40	–	[72] (1988)
Fluorinated graphite	$AlCl_3$-[BIM][Br] r = 0.5	0.6	75	40	3	300	–	[118] (2013)
Pyrolytic graphite	$AlCl_3$-[EMIm]Cl r = 1.3	1.8	98.1% ±0.4	>200	1	60–66	40	[43] (2015)
Natural graphite	$AlCl_3$-[EMIm]Cl r = 1.3	1.8	–	–	1	60–66	40	[43] (2015)
Graphitic foam	$AlCl_3$-[EMIm]Cl r = 1.3	1.7	97% ±2.3	7500	75	60	40	[43] (2015)
Kish graphite flakes	$AlCl_3$-[EMIm]Cl r = 2	1.8	–	200	67	142	65	[114] (2017)
Natural graphite flakes	$AlCl_3$-[EMIm]Cl r = 2	1.8	Up to 99	100	7.9	124	62	[42] (2017)
Natural graphite flakes	$AlCl_3$-[EMIm]Cl r = 1.3	2.1	99	6000	6	110	69	[120] (2017)
Pyrolytic graphite	$AlCl_3$-[EMIm]Cl r = 1.5	1.9	96–99	2000	1.3	75	–	[119] (2017)
Zeolite-templated carbon	$AlCl_3$-[EMIm]Cl r = 1.3	1.05	99–100	1000	4.5	175	64	[75] (2017)

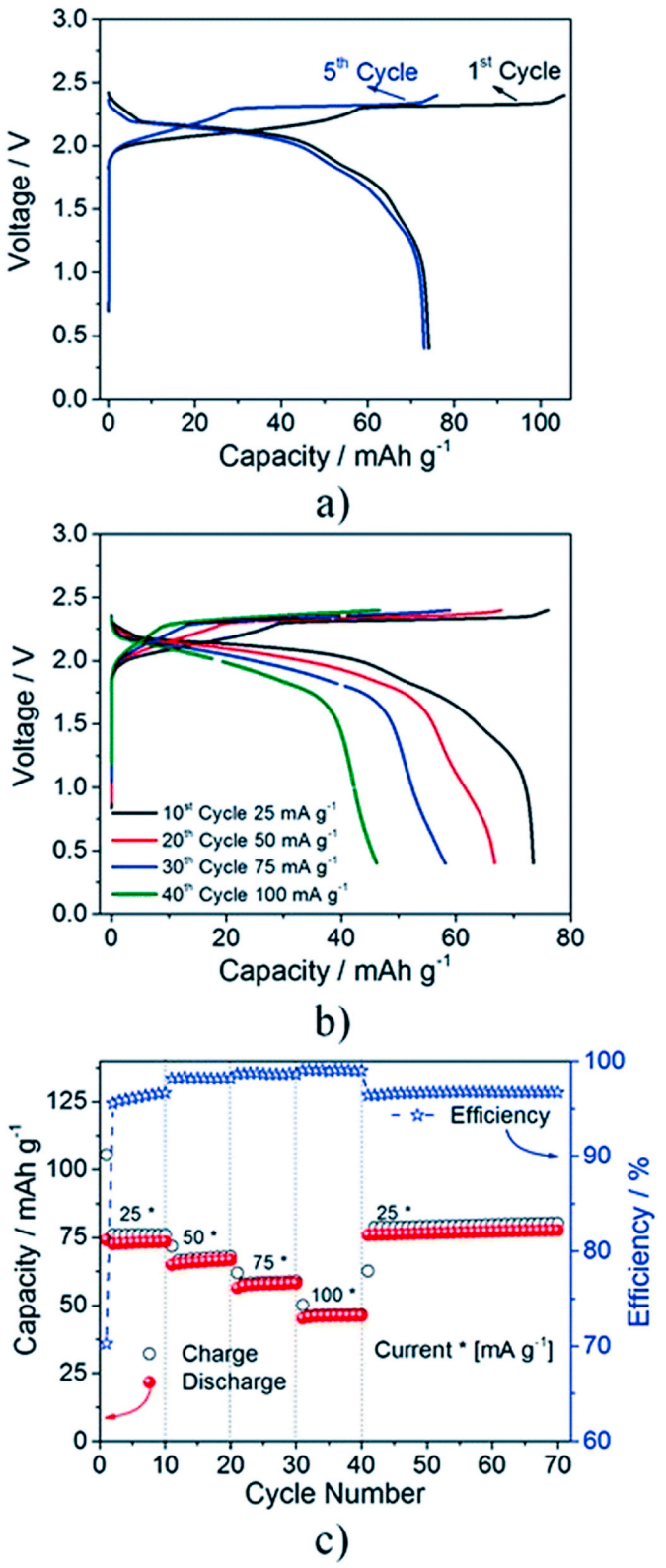

Fig. 7. Charge/discharge curve of an aluminium-graphite battery showing discharge potential at 1st and 5th cycles (a), discharge potential at different current densities (b) and coulombic efficiencies and specific charge/discharge capacities at different current densities. (Reproduced under Creative Commons 3.0 [https://creativecommons.org/licenses/by/3.0/] from Ref. [119]).

This wide range of results suggests that a consensus has not yet been reached on the mechanism of $AlCl_4^-$ storage in graphite; this is partly because of comparison of models and experimental results carried out on different forms of graphite. Modelling has also not yet accounted for the cycling effects on graphite: initial cycles demonstrate poor reversibility and capacity [72,119], with initially large and then gradual improvements over subsequent cycles, as chloroaluminate anions and $EMIm^+$ cations forcibly alter the microstructure, with some remaining in the positive electrode permanently. The scale of the improvement can be as large as 45 mAh g^{-1} on the first cycle to 65 mAh g^{-1} on the 500th cycle [119].

While positive electrode capacity and discharge potential are highest at around $r = 1.3–1.5$ [42,43,114], this is mooted by the requirement to cycle between $r = 2$ and $r = 1.1$ to maximise specific energy. The use of $r = 2$ electrolyte is required to achieve 65 Wh kg^{-1}, which is close to the theoretical maximum possible using aluminium-graphite batteries with RTIL electrolyte [42,114]. The future of graphite intercalation looks to more exotic architectures of carbon to achieve greater specific energy. One potentially promising area of research is single walled carbon nanotubes, which have the advantage of potentially being able to be sized optimally for $AlCl_4^-$ intercalation. Modelling has indicated the potential for a 275 mAh g^{-1} specific capacity [128]. However, the improvements achievable from novel carbon architectures are marginal due to the dependency of the specific energy on the amount of electrolyte present. Currently, flaky graphite positive electrodes offer the best performance overall in non-aqueous aluminium batteries due to their high average discharge potential, long cycle life, and reasonable specific capacity.

5.1.2. *Conductive polymers*

The field of conductive polymer research has been active for more than 40 years, since it was discovered that conjugated polyacetylene chains had semiconductor behaviour which could be enhanced via exposure to chlorine or bromine gas [129]. While polyacetylene was the first to be discovered, it was unstable in oxygen, and experienced decreasing conductivity with time. Further development led to (amongst others) the more stable polypyrrole and polythiophene, and then to poly-3,4-ethylenedioxythiophene (PEDOT). Conductive polymers have the advantage of low density compared to metals (1.46 g cm^{-3} for PEDOT relative to 8.96 g cm^{-3} for copper), offering the opportunity for high specific energy electrodes [130]. So far, conducting polymers have found applications in organic solar cells, organic light emitting diodes, and various kinds of sensors and processors, due to the combination of optical and electrical characteristics [131]. PEDOT is also showing promise in supercapacitors [132].

Conductive polymers store charge via oxidation of the pi-conjugated carbon backbone. As electrons are removed, the charges localise at specific points along the polymer chain due to energetically favourable relaxation of the molecular structure; these ‘defects’ cause geometry deviations from the equilibrium neutral geometry that each affect several chain units. However, they remain mobile. When anions are introduced however, they coordinate near the polymer (Fig. 8 indicates the typical arrangement of an $AlCl_4^-$ anion near a PEDOT chain) to counterbalance the missing electrons and balance the polymer charge. This effectively pins the localised charges in place, helping to spread the charges throughout the polymer bulk and increasing conductivity, which occurs due to electron transport between defects [133]. The exact mechanism of electrical conduction in polymers is not entirely defined, partly because it actually involves several mechanisms [134–136]. Fig. 9 illustrates the storage of $AlCl_4^-$ in PEDOT, while the reaction is given in Equation (9) [95]:

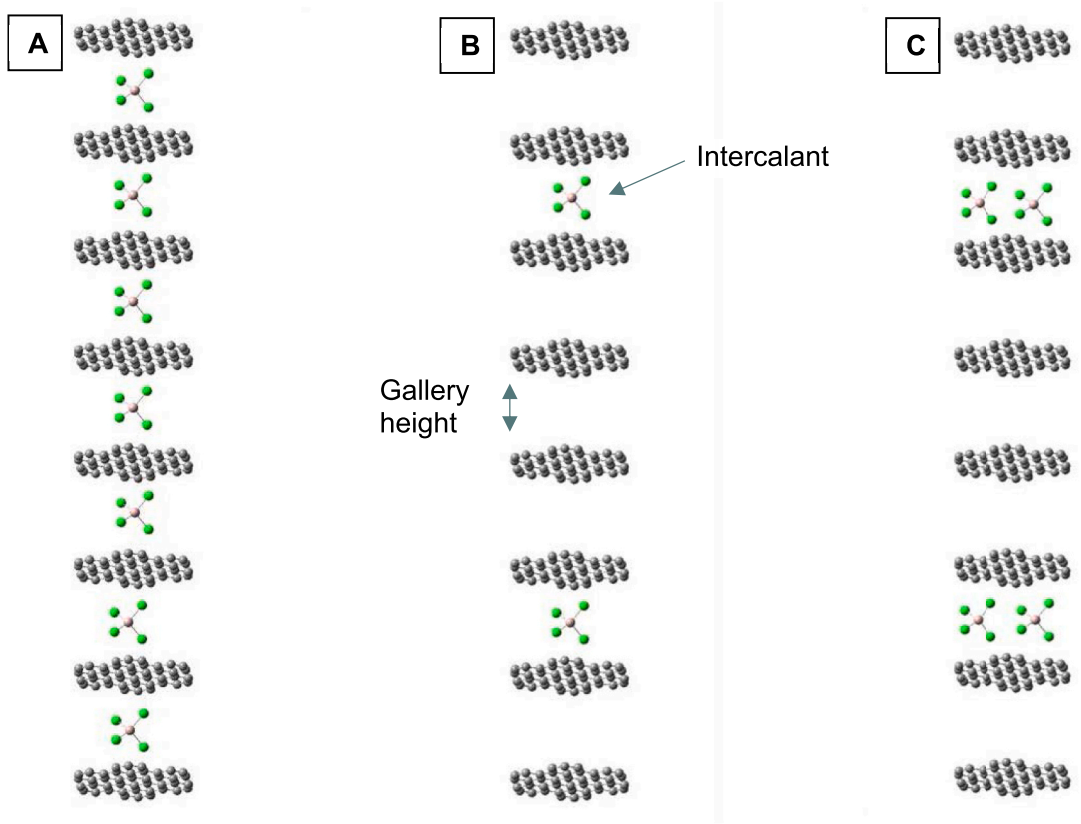

Fig. 8. A) Stage 1 single layer intercalation of graphite, B) Stage 4 single layer intercalation of graphite, C) Stage 4 double layer intercalation of graphite [120] (molecules drawn using Gaussview/Gaussian [44]).

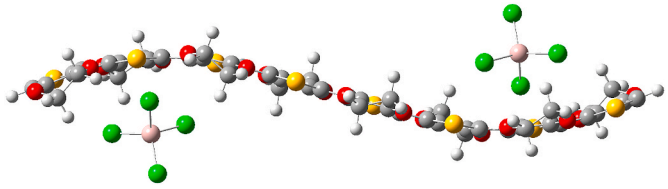

Fig. 9. *Coordination of $AlCl_4^-$ anions near the sulphur atoms in the PEDOT chain. Molecule optimized and visualized using Gaussview/Gaussian at the B3LYP 6-31+G (d) theory level with Grimme's D3(BJ) dispersion* corrections [44,137].

$$3[MonomerUnit]_{\alpha}+4Al_2Cl_7^- \underset{discharge}{\overset{charge}{\rightleftharpoons}} 3[MonomerUnit]_{\alpha}AlCl_4^- + Al + 4AlCl_4^-$$

Equation 9

The possible range of concentration of inserted anions in a conducting polymer is large (possibly up to one anion per chain unit) [46,138], which allows a conducting polymer to store anions in a cathodic capacity [2]. Anion insertion into polymers is analogous to anion intercalation into graphite. Intercalation involves storage of an ion in specific sites in the crystal lattice or between layers of the material, whereas insertion involves storage near preferential locations on a polymer which may have an amorphous or partially crystalline structure. Polypyrrole, polythiophene and PEDOT have all been trialled in non-aqueous aluminium batteries and are discussed here [13,46]. PEDOT is synthesized from polythiophene. Thiophene is sourced from fossil fuels, from which it is removed by necessity to reduce sulphur emissions; therefore it is abundant, maintaining the benefits of aluminium batteries [139,140].

5.1.2.1. Polypyrrole and polythiophene. Hudak [13] investigated polypyrrole and polythiophene electrodes with an aluminium negative electrode and $AlCl_3$-[EMIm]Cl $r = 1.5$ electrolyte. Polypyrrole was electropolymerized and the counterions inserted in the same electrolyte using galvanostatic polarization. Elemental analysis was used to determine the molar ratio of chlorine to aluminium, and the ratio of the two chloroaluminate species present was calculated to be 77.7 mol % $AlCl_4^-$ and 22.3 mol % $Al_2Cl_7^-$. Furthermore, the percentage of anions relative to polymer units was found to be 24.6%. The polymers stored charge via a faradaic redox reaction until the redox potential of this process was exceeded. Above this, non-faradaic charge storage occurred, likely via a double-layer capacitor effect – in its neutrally charged form, the polymer is non-conductive, so non-faradaic charge storage can only take place once it has been oxidised. In addition to having better coulombic efficiency (>98% *vs.* > 96%), polypyrrole withstood over-oxidation better than polythiophene, however, polythiophene had a slightly higher average discharge potential (1.47 V *vs.* 1.42 V). The charge/discharge is broadly reversible (>96% coulombic efficiency) so long as the discharge potential is kept between 0.1 and 2.0 V *vs.* Al|Al(III). Above 2.6 V, the authors proposed that the films reacted with the chloroaluminate species. Even above 1.5 V *vs.* Al|Al(III) however, some irreversibility was seen. In conclusion, maximum specific energies of 44.4 Wh kg^{-1} for polythiophene and 46.4 Wh kg^{-1} for polypyrrole were calculated based on the electrolyte and the active electrode mass. The specific capacity of the polymer films was estimated to be 30–100 mAh g^{-1}, meaning that polypyrrole and polythiophene fall behind graphite flakes in terms of both average discharge potential and specific positive electrode capacity [13].

5.1.2.2. PEDOT. Poly(3,4-ethylenedioxythiophene) (PEDOT) (Fig. 8), patented in 1988 [141], was initially developed to overcome the toxicity risks of polyaniline chemistry while still being soluble and fusible.

PEDOT is extremely stable when charged and discharged, and has a moderate band gap [142,143]. It can be synthesized to have higher potentials in an aluminium battery than polypyrrole or polythiophene [144]. PEDOT has found application in anti-static coatings, supercapacitor electrodes, hole injection layers in OLEDs and organic solar cells [145]. PEDOT can either be made into a free-standing film [77,146,147], or it can be combined with other materials such as non-conductive polymers to improve its mechanical properties [130]. All these properties point to PEDOT as a candidate positive electrode for aluminium batteries.

A PEDOT positive electrode can be electropolymerized at up to 2.3 V *vs.* Al|Al(III) in $AlCl_3$-[EMIm]Cl before reaching the electrolytic breakdown of the ionic liquid, showing that it may have the potential to withstand even higher potentials if a suitable electrolyte is found. The charge/discharge potential of the synthesized electrode in a battery is limited by the maximum potential reached during electropolymerization. Higher potential electropolymerization is theorized to lead to a denser, cross-linked network of longer PEDOT chains which have higher potential anion insertion sites. The mechanism is not yet confirmed [80]; it is anticipated that computational techniques may reveal the mechanisms behind this phenomenon.

The discharged PEDOT film has a granular structure. As it is charged, it undergoes morphological changes, where the grains first expand, then merge. When the electrode is discharged, a new granular structure is formed. This mechanism is illustrated in Fig. 10 [148].

Improved structural stability and surface area of a PEDOT electrode can be achieved by using a three-dimensional reticulated vitreous carbon (RVC) substrate instead of planar vitreous carbon. The PEDOT forms a uniform film over the surface of the RVC without blocking the holes in the macrostructure, allowing for much greater surface area and improved mechanical properties relative to a planar film. The electropolymerization process was successfully reproduced on 3D RVC. The optimum method is cyclic voltammetry, from −0.5 V to 2.6 V *vs.* Al|Al (III). This is hypothesised to be due to the formation of anion paths in the polymer during repeated cycling, whereas at constant current or potential, there is no anion removal during electropolymerization. With this method, the PEDOT electrode has around 45% higher capacity than the planar carbon electrode, and has demonstrated structural stability over 250 cycles, with a coulombic efficiency of 94%. The use of a porous carbon current substrate is convenient for battery packaging, because it provides a fixed macroscopic geometry that does not change during charging – the PEDOT can expand within the pores inside the carbon. However, the latest work still demonstrates large pores of unused space in the RVC substrate, and the opportunity for significant further optimisation [144].

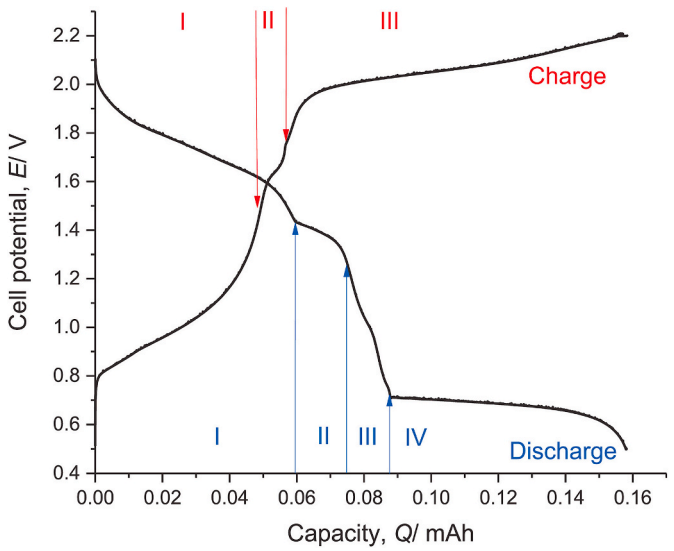

Fig. 11. Charge/discharge of an aluminium-PEDOT battery, charged at 0.1 mA to 2.2 V and discharged at −0.1 mA to 0.5 V at 25 °C. (Reproduced with permission from the Journal of Energy Storage [46]).

The charge and discharge curve of an aluminium-PEDOT battery is

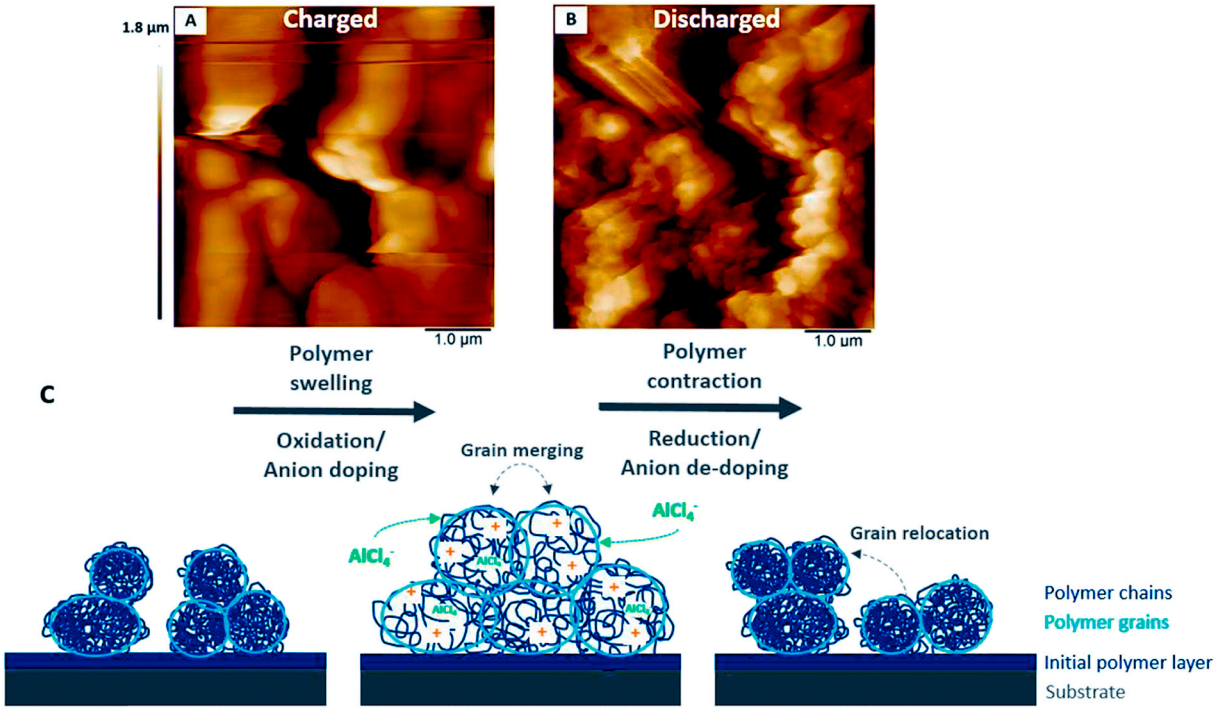

Fig. 10. Mechanism of charge storage in PEDOT (reproduced under Creative Commons 3.0 [https://creativecommons.org/licenses/by/3.0/] from Refs. [148]). AFM images of PEDOT in monomer-free Lewis neutral EMImCl–$AlCl_3$ in the fully (A) charged and (B) discharged states and (C) schematic model of the morphological changes of a conductive polymer in an ionic liquid during charging (oxidation, anion insertion) and discharging (reduction, anion removal).

shown in Fig. 11. The discharged PEDOT film is compact and cannot accept the insertion of anions; this is section I and corresponds to a surface charging mechanism. The PEDOT oxidises and swells during charging, and once it reaches section III the swelling means it can accept large-scale insertion of anions. Section II corresponds to a transition between these two stages [46].

Overall, PEDOT appears to offer an improvement over polypyrrole or polythiophene due to increased chemical stability (it is less vulnerable to reacting at high potentials), and higher specific capacity of the positive electrode (192 mAh g^{-1} relative to 30–100 mAh g^{-1}). Recent work indicates that the specific capacity of PEDOT is higher than graphite (191 mAh g^{-1} *vs.* 142 mAh g^{-1}), but the reduced average discharge potential of 1.3 V means the specific energy of the whole battery is lower (50 Wh kg^{-1} *vs.* 65 Wh kg^{-1}) [13,43,46,114].

5.1.3. Iron chloride

There are potential benefits to storing Cl^- instead of $AlCl_4^-$, chiefly that Cl^- is smaller [2,72], assuming that Cl^- can be extracted from $Al_2Cl_7^-$ species in the acidic electrolyte. This would have to be by preferential reaction as free Cl^- is not present in acidic chloroaluminate electrolytes; researchers who intended to intercalate Cl^- ions into graphite or conductive polymers either did not carry out analysis to prove Cl^- had been stored [72] or later found that it was chloroaluminate anions that actually provided the charge storage [2]. Perhaps the most persuasive example of Cl^- storage used an $FeCl_3$ positive electrode that was reported to convert to $FeCl_2$ on discharge. The $FeCl_2$ was impregnated in reticulated vitreous carbon in $AlCl_3$-[EMIm]Cl at a 1.38 M ratio. A stainless steel current collector was used. A full cell discharge potential of 1.85 V *vs.* Al|Al(III) was found, and the researchers proposed Equation (10) as the cell reaction [45]:

$$Al + AlCl_4^- + 3FeCl_3 \rightleftharpoons Al_2Cl_7^- + 3FeCl_2 \quad \text{Equation 10}$$

However, the positive electrode was not analysed post-discharge to assess if $FeCl_2$ to $FeCl_3$ had actually occurred [45]. Stainless steel is also known to be electroactive in $AlCl_3$-[EMIm]Cl, which may also have contributed [149]. The achieved energy density was not stated, and because the positive electrode was soluble in the electrolyte, the battery was prone to self-discharge, making it unsuitable for further investigation [45].

5.2. Positive electrodes storing Al(III)

The materials discussed in this section have been claimed to intercalate Al(III) directly. While some researchers reviewing the literature up until very recently (2017) did not consider Al(III) to ever have been proved to be successfully intercalated into any positive electrode material [75,149], we believe there is some evidence that Al(III) intercalation has taken place despite the difficulties of intercalating polyvalent ions [13]. Because the electrolyte in these systems is not depleted during charge or discharge, these papers tend to use RTIL electrolytes with *r* of 1.1–1.3, close to minimum Lewis acidity required aluminium deposition. In this section, sulphur, vanadium-based positive electrodes, and transition metal sulphides are discussed. On a side note, Al(III) intercalation has been successfully shown in aqueous aluminium batteries [150], however, this material has not been demonstrated in ionic liquid electrolytes [151].

5.2.1. Sulphur

As a positive electrode material operating by a conversion reaction (stored ions react to form a new chemical phase with the positive electrode), sulphur is now being considered for use in aluminium batteries. As expected, the latest research on aluminium-sulphur makes use of chloroaluminate ionic liquids [116,152–154]. The reaction is as shown in Equation (11):

$$2Al + 14AlCl_4^- + Al_2S_3 \rightleftharpoons 8Al_2Cl_7^- + 3S \quad \text{Equation 11}$$

For lithium-ion and sodium-ion batteries, sulphur is one of the most promising materials for moving forwards in terms of specific energy from the current generation of metal oxide positive electrodes. Although it offers increased specific energy and is highly abundant, it has poorer energy density than metal oxide positive electrodes. Sulphur has also been attempted as a positive electrode for aluminium batteries due to its theoretical specific energy (based on total electrode mass) of 1340 Wh kg^{-1} based on a discharge potential of 1.1–1.25 V *vs.* Al|Al(III) – significantly higher than current lithium-ion batteries [116]. A primary aluminium-sulphur battery has been demonstrated attaining very close to this theoretical specific energy [152]. However, as with all other positive electrodes that store aluminium, aluminium-sulphur is characterised by poor cycle life (a few tens of cycles compared to thousands for positive electrodes storing chloroaluminate anions). To improve the kinetics of the AlS_x oxidation reaction, various strategies have been attempted. These include encapsulating sulphur into the micropores (2 nm) of activated carbon, achieving a cycle life of 20 with capacity retention of 65% [116], and incorporating Li^+ ions into the electrolyte, achieving a cycle life of 50 cycles with a capacity retention of 60% [154].

5.2.2. Vanadium-containing positive electrodes

5.2.2.1. Li_3VO_4. Li_3VO_4 consists of a hollow 3D structure with pores that are intermediate in size between Al(III) and $AlCl_4^-$ into which it has been theorized that Al(III) could be inserted via intercalation according to the following full-cell reaction shown in Equation (12):

$$Li_3VO_4 + xAl \rightleftharpoons Al_xLi_3VO_4 \quad \text{Equation 12}$$

An aluminium battery with $AlCl_3$-[EMIm]Cl electrolyte and Li_3VO_4 positive electrode was reported with an initial discharge capacity of 137 mAh g^{-1} which dropped to 48 mAh g^{-1} after 100 cycles. After the initial loss of capacity was accounted for, the battery was reported to have ~100% coulombic efficiency at an average cell discharge potential of <1 V *vs.* Al|Al(III) [38]. This study raises several questions. A stainless steel current collector was used, known to exhibit redox behaviour due to Fe and Cr redox reactions, producing similar discharge potentials to those found here [149]. It is suggested that V^{4+} is oxidised to V^{5+} during the charge process. Additionally, the Li_3VO_4 was completely coated with approximately 5 nm of carbon, both graphitic and disordered types, strongly indicating the potential for some chloroaluminate redox reaction with graphite. The initial charge behaviour indicates that the structure has been intercalated and altered by the presence of anions, suggesting a mixture of graphitic storage and stainless steel electro-activity. Finally, the use of vanadium and lithium, neither of which are abundant elements, lowers the appeal of this positive electrode material for post-lithium batteries [38].

5.2.2.2. V_2O_5. V_2O_5 is one of the more controversial positive electrode materials for aluminium batteries, with researchers arguing both for and against the possible storage of Al(III). In this review, it is argued that there is some evidence for Al(III) intercalation in V_2O_5, but a low average discharge potential of less than 0.6 V *vs.* Al|Al(III) limits its use as a battery system. The cell reaction is as shown in Equation (13) [115]:

$$V_2O_5 + Al \rightleftharpoons AlV_2O_5 \quad \text{Equation 13}$$

The reversible intercalation of Al(III), Mg(II) and Zn(II) into V_2O_5 was shown in a 1998 study on V_2O_5 aerogels. Initial intercalation was carried out by immersing aerogel electrodes for one week into dibutylmagnesium, dimethylzinc or trimethylaluminium for Mg^{2+}, Zn^{2+} or Al^{3+} respectively, all in heptane solution. All demonstrated reversible electroactive behaviour [155].

In 2011, in one of the earliest studies on V_2O_5 in an aluminium battery [156], Jayaprakash et al. found that using V_2O_5 nanowires and a stainless steel current collector allowed for a battery system that

demonstrated a sharp drop in cell discharge potential from 1.8 V *vs.* Al|Al(III) open-circuit potential to a plateau of about 0.55 V *vs.* Al|Al(III). The capacity of the positive electrode was around 273 mAh g^{-1} after 20 cycles, which is a good capacity, although the poor discharge potential means that the overall specific energy was not high. This paper used an $r = 1.1$ $AlCl_3$-[EMIm]Cl electrolyte [156]. Reed et al. [149] attempted in 2013 to replicate the battery system and found that the low discharge potential (0.6 V *vs.* Al|Al(III)) achieved with V_2O_5 in a Swagelok cell was attributable to reactions involving the iron and chromium in the stainless steel current collector, destroying the cell via dendrite growth after just 20 cycles. This was supported by the fact that V_2O_5 demonstrated no electrochemical activity in a battery when combined with an unreactive platinum current collector.

More recently in 2015, Wang et al. [115] demonstrated that V_2O_5 deposited on a Ni foam current collector is electroactive, while Ni foam on its own is not. Although the cells were charged to 2.5 V *vs.* Al|Al(III), the potential dropped rapidly during discharge limiting the average discharge potential, as for Jayaprakash et al., to 0.6 V *vs.* Al|Al(III). This perhaps indicates that Al(III) or chloroaluminate species are forming stable compounds at a potential of only 0.6 V *vs.* Al/Al(III). The cell had an initial specific discharge capacity based on positive electrode mass of 239 mAh g^{-1} which reduces by around 20% over the first five cycles. The electrolyte was r = 1.1 $AlCl_3$-[BMIM]Cl, the minimum value at which $Al_2Cl_7^-$ is present for aluminium deposition. Though it was shown that the V was oxidised from V^{4+} to V^{5+} during charging, this could account for chloroaluminate species intercalation during charging, and no conclusive evidence of Al(III) intercalation is presented.

Chiku et al. [157] found that using a V_2O_5 positive electrode with an ionic liquid electrolyte consisting of $AlCl_3$, dipropylsulfone and toluene in a 1:10:5 ratio, gave a 1st cycle discharge capacity of 150 mAh g^{-1} V_2O_5, followed by 100 mAh g^{-1} on the 15th cycle with good coulombic efficiency. A closer analysis found that before cycling, only V^{5+} was present, but this was reduced to V^{3+} and V^{4+} during discharging. A molybdenum current collector was used, having been shown to be unreactive in the relevant discharge potential range in the electrolyte. Clearly, V_2O_5 is electroactive, and the capacity obtained is approximately matched to the theoretical calculation. The authors concluded that V_2O_5 is electroactive and might able to store Al(III), but in a battery system, it provides a steeply sloping and low average discharge potential profile, limiting its use based on current progress.

5.2.2.3. VO_2. In 2013, Jiang et al. [41] investigated a VO_2 material with a stainless steel current collector for the positive electrode. They use computational modelling to demonstrate the potential intercalation behaviour of aluminium in the VO_2 matrix via the following reaction (x is the experimentally found value) shown in Equation (14):

$$VO_2 + xAl \rightleftharpoons Al_xVO_2 \quad (x \sim 0.17) \qquad \text{Equation 14}$$

They found that all formation energies were negative, indicating that intercalation was possible and that intercalating a small number of aluminium atoms was well tolerated by the matrix, but above that, the bonds started to bend and break. They concluded that aluminium could not replace V in the matrix due to a positive energy of formation. The positive electrode maintains a capacity of over 100 mAh g^{-1} in testing based on the mass of the positive electrode alone, but the discharge potential is low at around 0.55 V *vs.* Al|Al(III). The electrolyte was $r = 1$ $AlCl_3$-[BMIM]Cl and the authors report a 48 Wh kg^{-1} specific energy [41]. However, as previously discussed the use of stainless steel as a current collector means the results must be treated with caution [149].

In summary, all attempts to use vanadium-containing positive electrodes have resulted in low discharge potentials of less than 0.6 V, resulting in specific energy values that fall behind aluminium-graphite (48 Wh kg^{-1} *vs.* 65 Wh kg^{-1}) [41,43,114].

5.2.3. Transition metal sulphides

Conversion electrodes use chemical reactions between the positive electrode and the intercalating species to form entirely new products stored together at the positive electrode [158]. Conversion electrodes based on fluorides, oxides and sulphides have been explored for aluminium batteries, but fluorides and oxides form very strong ionic bond with aluminium, causing high binding energies. Sulphides, which form weaker ionic bonds with aluminium, remain as positive electrode materials of interest [39].

5.2.3.1. TiS_2. In 2017, Geng et al. [40] investigated a transition metal sulphide, TiS_2, which has a more polarizable anionic structure than transition metal oxides like V_2O_5, and therefore should have reduced barriers to the transport of multivalent ions. Storage of aluminium was investigated from an $r = 1.5$ $AlCl_3$-1-butyl-3-methylimidazolium chloride electrolyte. Reversibility was demonstrated for both layered TiS_2 and spinel-based cubic $Cu_{0.31}Ti_2S_4$, and it was shown that Al(III) resided in the octahedral sites in the layered TiS_2. While Al(III) intercalation was demonstrated, its passage through the crystal structure was slow, and the binding energy of aluminium in TiS_2 was still high enough to cause low discharge potential. Experimentally, for the better performing layered TiS_2, a highly sloping discharge potential with an average value of less than 1 V *vs.* Al|Al(III) was found with a capacity of about 70 mA h g^{-1} (based on positive electrode mass) after several cycles, indicating that around 11% of the available octahedral intercalation sites were taken by Al(III). The positive electrode initially demonstrated poor discharge capacity and coulombic efficiency, and both improved on subsequent cycles to a stable value. However, while specific energy is not calculated, both the specific capacity of the TiS_2 electrode and its average discharge potential fall far behind Al-graphite (70 mAh g^{-1} *vs.* 142 mAh g^{-1} and 1 V *vs.* 1.77 V respectively [114].

5.2.3.2. Ni_3S_2 on graphene microflakes. In 2016, Yu et al. [117] investigated Ni_3S_2 on graphene microflakes in an $AlCl_3$-[EMIm]Cl electrolyte. With a discharge potential of around 1 V *vs.* Al|Al(III), the discharge capacity remained over 60 mAh g^{-1} (based on positive electrode mass) after 100 cycles, with an initial charge/discharge capacity of 300 and 235 mAh g^{-1} respectively. These results are similar to those reported for TiS_2, and the same comparisons to aluminium-graphite apply.

5.2.3.3. FeS_2. Also in 2016, Mori et al. [39] investigated the theoretical mechanism for Al(III) intercalation in FeS_2 – a transition metal sulphide that has been used successfully in lithium and sodium battery positive electrodes. They used an $r = 2$ $AlCl_3$-[EMIm]Cl electrolyte. FeS_2 has the advantage of being naturally abundant. For lithium-ions, the FeS_2 goes through an intermediate, layered phase of Li_2FeS_2 before reaching its fully charged configuration. For aluminium however, the high charge density makes this intermediate phase unstable, and so diffusion into the bulk is required. The cell reaction is shown in Equation (15):

$$FeS_2 + \frac{2}{3}Al \rightleftharpoons FeS + \frac{1}{3}Al_2S_3 \qquad \text{Equation 15}$$

FeS_2 becomes FeS and Al_2S_3 - a conversion reaction. In practise, sulphide dissolution occurs, causing poor cycling stability, and low discharge potential results from the difficulty of diffusing Al(III) through bulk FeS_2. Nevertheless, the theoretical mechanism for intercalation was successfully demonstrated via XRD and XAS measurements. Future work includes combining with a nanostructure carbon substrate to provide diffusion paths and increased surface area.

5.2.4. Anthraquinone

The aluminium-anthraquinone (AQ) battery uses an anthraquinone-based poly(antraquinoyl sulfide) (PAQS) positive electrode to store charge and a $r = 1.5$ $AlCl_3$-[EMIm]Cl electrolyte [159]. PAQS has previously been used for lithium batteries [160], where a discharge

potential of 2.2 V *vs.* Al|Al(III) has been achieved. For the AQ battery [159], XPS results were used to calculate that the major Al containing species must be $AlCl^{2+}$. However, as previously discussed, this species does not appear in the electrolyte. Instead, $AlCl_4^-$ and $Al_2Cl_7^-$ are present in $r = 1.5$ $AlCl_3$-[EMIm]Cl. Therefore, questions remain over the operation of the battery, which cast doubt over the quoted energy density of 101 Wh kg^{-1}; it is most likely that the Al-containing species are actually being stored. More than 60% of the initial capacity remains after 500 cycles, but this is not competitive with Al-graphite or Al-PEDOT batteries.

5.3. Current collectors

The use of acidic ionic liquid electrolyte in aluminium batteries means that care must be taken when selecting current collectors. Materials that are completely inactive in these systems include molybdenum, tungsten and platinum, but clearly these are not abundant or affordable [42]. Other commonly used equipment also cannot withstand these electrolytes [113]; states an experimental failure due to Celgard Swagelok separator corrosion. Even some binders are active – although PTFE is stable, PVDF reacts [115]. Carbon-coated aluminium foil [144] and carbon have been used successfully as anodic current collectors [161]. If the aluminium purity is extremely high (so as not to contaminate the electrolyte), it can act as its own current collector at the negative electrode, although it might seem prudent to use an unreactive current collector to minimise the risk of holes forming because of uneven dissolution of the electrode during discharge.

6. Summary and future perspective

Due to the particularly difficult challenge of finding positive electrodes that have good discharge potential and cycle life, the research focus is likely to remain towards those materials that store chloroaluminate species. No electrolytes have yet been shown to have a wider electrochemical window or better stability than $AlCl_3$-[EMIm]Cl. Forming a gel of this electrolyte is a very interesting research avenue, as it is the only obvious route for improving the electrochemical window of RTILs.

Deep eutectic solvents are of interest because some of them are cheap and particularly non-toxic. However, they offer a limited electrochemical stability window and composition range suitable for aluminium deposition, and because specific energy is such a key parameter for new energy storage, it seems unlikely that their cost and toxicity credentials can make up for their lack of performance. Entirely new DES with improved performance need to be discovered for them to gain relevance in non-aqueous aluminium batteries.

Graphite-based positive electrodes offer the best overall performance due to the stability and high average discharge potential. Cheap and relatively abundant graphite flakes seem to offer the best balance of performance and cost and achieve near the theoretical maximum in terms of specific energy and thousands of cycle lives [114]. Conducting polymers offer similar operation but average discharge potential and cycle life are lower than for graphite [13,46]. Elaborate structures such as carbon nanotubes may elicit marginal gains in the specific capacity of graphite electrodes, but these are unlikely to be economically justified considering the cost of developing carbon nanostructures compared to assembling graphite flakes. There may also be ways to improve the capacity of conducting polymer electrodes using refined electrosynthesis techniques, but again these improvements are likely to be marginal. Other positive electrode materials that store chloroaluminate species fall far behind graphite and conducting polymers. Positive electrode materials that store Al(III) offer much better theoretical performance but there is little evidence of this theoretical performance being achieved over a long cycle life; aluminium-sulphur probably appears most promising but still only maintains 60% of its capacity over 50 cycles [154].

Considering the highest achieved specific energy of 68 Wh kg^{-1}, and accounting for the extra mass involved in commercial packaging, current aluminium batteries may have sufficient specific energy to meet grid storage requirements. However, the cost of ionic liquids is a barrier to entering the market. Improved performance, cheaper electrolyte, or both, would help to improve prospects. If aluminium batteries could reach higher specific energies, perhaps greater than 200 Wh kg^{-1}, they might begin to compete in the electric vehicle market. They would still not compete with lithium ion batteries on specific energy, but might offer better charging time, affordability, environmental credentials and cycle life. Then, the technology might become optimal for applications demanding predictable length journeys with regular charging opportunities. Combined with an electric drive this could fulfil a huge number of mass transit applications globally, most of which are currently serviced by diesel engines. With these potential applications in mind, aluminium battery technology should be relentlessly pursued towards its theoretical performance limits, to ensure its full potential is realised as soon as possible in the quest to develop a sustainable future.

CRediT authorship contribution statement

Ben Craig: Conceptualization, Investigation, Writing - original draft. **Theresa Schoetz:** Writing - review & editing. **Andrew Cruden:** Writing - review & editing. **Carlos Ponce de Leon:** Writing - review & editing, Supervision.

Declaration of competing interest

The authors declare that they have no known competing financial interests or personal relationships that could have appeared to influence the work reported in this paper.

Acknowledgements

The authors acknowledge support from the International Consortium of Nanotechnologies (ICON) funded by Lloyd's Register Foundation [G0086], a charitable foundation which helps to protect life and property by supporting engineering-related education, public engagement and the application of research, and from the Engineering and Physical Sciences Research Council, through the Centre for Doctoral Training in Energy Storage and its Applications at the University of Southampton [EP/L016818/1].

References

[1] Becke AD. Density-functional thermochemistry. III. The role of exact exchange. J Chem Phys 1993;98:5648–52.
[2] Schoetz T, Ueda M, Bund A, Ponce de Leon C. Preparation and characterization of a rechargeable battery based on poly-(3,4-ethylenedioxythiophene) and aluminum in ionic liquids. J Solid State Electrochem 2017;21:3237–46.
[3] Nykvist B, Sprei F, Nilsson M. Assessing the progress toward lower priced long range battery electric vehicles. Energy Pol 2019;124:144–55.
[4] Statista. Projected battery costs as a share of large battery electric vehicle costs from 2016 to 2030. Statista; 2018.
[5] She Z-Y, Sun Qing, Ma J-J, Xie B-C. What are the barriers to widespread adoption of battery electric vehicles? A survey of public perception in Tianjin, China. Transport Pol 2017;56:29–40.
[6] Diouf B, Pode R. Potential of lithium-ion batteries in renewable energy. Renew Energy 2015;76:375–80.
[7] Kavanagh L, Keohane J, Garcia Cabellos G, Lloyd A, Cleary J. Global lithium sources—Industrial Use and future in the electric vehicle Industry: a review. Resources 2018;7.
[8] Walt V, Meyer S. Blood, Sweat and batteries. Fortune2018.
[9] Zhang W, Xu C, He W, Li G, Huang J. A review on management of spent lithium ion batteries and strategy for resource recycling of all components from them. Waste Manag Res 2018;36:99–112.
[10] Manthiram A. Materials challenges and Opportunities of lithium ion batteries. J Phys Chem Lett 2011;2:176–84.
[11] Dehghani-Sanij AR, Tharumalingam E, Dusseault MB, Fraser R. Study of energy storage systems and environmental challenges of batteries. Renew Sustain Energy Rev 2019;104:192–208.

[12] Finegan DP, Scheel M, Robinson JB, Tjaden B, Hunt I, Mason TJ, et al. In-operando high-speed tomography of lithium-ion batteries during thermal runaway. Nat Commun 2015;6:6924.
[13] Hudak NS. Chloroaluminate-doped conducting polymers as positive electrodes in rechargeable aluminum batteries. J Phys Chem C 2014;118:5203–15.
[14] Li Q, Bjerrum NJ. Aluminum as anode for energy storage and conversion: a review. J Power Sources 2002;110:1–10.
[15] Holland A, McKerracher RD, Cruden A, Wills RGA. An aluminium battery operating with an aqueous electrolyte. J Appl Electrochem 2018;48:243–50.
[16] Chen H, Xu H, Zheng B, Wang S, Huang T, Guo F, et al. Oxide film efficiently Suppresses dendrite growth in aluminum-ion battery. ACS Appl Mater Interfaces 2017;9:22628–34.
[17] Lin D, Liu Y, Cui Y. Reviving the lithium metal anode for high-energy batteries. Nat Nanotechnol 2017;12:194–206.
[18] Haering; Rudolph R. SJAR, Brandt; Klaus Lithium molybdenum disulphide battery cathode. In: USPTO, editor. H01M 4/58 (20060101); H01M 10/40 (20060101); H01M 10/42 (20060101); H01M 4/36 (20060101); H01M 4/02 (20060101); H01M 10/44 (20060101); H01M 10/36 (20060101); H01M 006/14 ed. US1980.
[19] Galiński M, Lewandowski A, Stępniak I. Ionic liquids as electrolytes. Electrochim Acta 2006;51:5567–80.
[20] Committee TGAR. Global aluminium recycling: a Cornerstone of sustainable development. International Aluminium Institute; 2009.
[21] Li L, Zheng Y, Zhang S, Yang J, Shao Z, Guo Z. Recent progress on sodium ion batteries: potential high-performance anodes. Energy Environ Sci 2018;11:2310–40.
[22] Quinn JB, Waldmann T, Richter K, Kasper M, Wohlfahrt-Mehrens M. Energy density of cylindrical Li-ion cells: a comparison of commercial 18650 to the 21700 cells. J Electrochem Soc 2018;165:A3284–91.
[23] Hwang JY, Myung ST, Sun YK. Sodium-ion batteries: present and future. Chem Soc Rev 2017;46:3529–614.
[24] Ponrouch A, Palacin MR. On the road toward calcium-based batteries. Current Opinion in Electrochemistry 2018;9:1–7.
[25] Mainar AR, Iruin E, Colmenares LC, Kvasha A, de Meatza I, Bengoechea M, et al. An overview of progress in electrolytes for secondary zinc-air batteries and other storage systems based on zinc. Journal of Energy Storage 2018;15:304–28.
[26] Zhang Y, Chen Z, Qiu H, Yang W, Zhao Z, Zhao J, et al. Pursuit of reversible Zn electrochemistry: a time-honored challenge towards low-cost and green energy storage. NPG Asia Mater 2020;12.
[27] Diggle J, Despic A, Bockris J. The mechanism of the dendritic Electrocrystallization of zinc. J Electrochem Soc 1969;116:1503–14.
[28] Higashi S, Lee SW, Lee JS, Takechi K, Cui Y. Avoiding short circuits from zinc metal dendrites in anode by backside-plating configuration. Nat Commun 2016;7:11801.
[29] Yu W, Shang W, Xiao X, Tan P, Chen B, Wu Z, et al. Achieving a stable zinc electrode with ultralong cycle life by implementing a flowing electrolyte. J Power Sources 2020:453.
[30] Muldoon J, Bucur CB, Gregory T. Fervent Hype behind magnesium batteries: an open Call to Synthetic Chemists-electrolytes and cathodes needed. Angew Chem Int Ed Engl 2017;56:12064–84.
[31] Liu J, Xu C, Chen Z, Ni S, Shen ZX. Progress in aqueous rechargeable batteries. Green Energy & Environment 2018;3:20–41.
[32] Das SK, Mahapatra S, Lahan H. Aluminium-ion batteries: developments and challenges. J Mater Chem 2017;5:6347–67.
[33] Zhao Y, VanderNoot T. Review: electrodeposition of aluminium from nonaqueous organic electrolytic systems and room temperature molten salts. Electrochemica Acta 1997;42:3–13.
[34] Pan W, Wang Y, Zhang Y, Kwok HYH, Wu M, Zhao X, et al. A low-cost and dendrite-free rechargeable aluminium-ion battery with superior performance. J Mater Chem 2019;7:17420–5.
[35] Egan DR, Ponce de León C, Wood RJK, Jones RL, Stokes KR, Walsh FC. Developments in electrode materials and electrolytes for aluminium–air batteries. J Power Sources 2013;236:293–310.
[36] Wang H-F, Xu Q. Materials design for rechargeable metal-air batteries. Matter 2019;1:565–95.
[37] Manthiram A. An outlook on lithium ion battery technology. ACS Cent Sci 2017;3:1063–9.
[38] Jiang J, Li H, Huang J, Li K, Zeng J, Yang Y, et al. Investigation of the reversible intercalation/deintercalation of Al into the novel Li_3VO_4@C Microsphere composite cathode material for aluminum-ion batteries. ACS Appl Mater Interfaces 2017;9:28486–94.
[39] Mori T, Orikasa Y, Nakanishi K, Kezheng C, Hattori M, Ohta T, et al. Discharge/charge reaction mechanisms of FeS_2 cathode material for aluminum rechargeable batteries at 55°C. J Power Sources 2016;313:9–14.
[40] Geng L, Scheifers JP, Fu C, Zhang J, Bpt Fokwa, Guo J. Titanium sulfides as intercalation-type cathode materials for rechargeable aluminum batteries. ACS Appl Mater Interfaces 2017;9:21251–7.
[41] Wang W, Jiang B, Xiong W, Sun H, Lin Z, Hu L, et al. A new cathode material for super-valent battery based on aluminium ion intercalation and deintercalation. Sci Rep 2013;3:3383.
[42] Kravchyk KV, Wang S, Piveteau L, Kovalenko MV. Efficient aluminum chloride–natural graphite battery. Chem Mater 2017;29:4484–92.
[43] Lin MC, Gong M, Lu B, Wu Y, Wang DY, Guan M, et al. An ultrafast rechargeable aluminium-ion battery. Nature 2015;520:325–8.
[44] Frisch MJ, Trucks GW, Schlegel HB, G. E. Scuseria, Robb MA, Cheeseman JR, et al. Gaussian 09, Revision C.01. Gaussian, Inc. Wallingford CT2010.
[45] Donahue F, Mancini S, Simonsen L. Secondary aluminium-iron (III) chloride batteries with a low temperature molten salt electrolyte. J Appl Electrochem 1992;22:230–4.
[46] Schoetz T, Craig B, Ponce de Leon C, Bund A, Ueda M, Low CTJ. Aluminium-poly (3,4-ethylenedioxythiophene) rechargeable battery with ionic liquid electrolyte. Journal of Energy Storage 2020;28:101176–85.
[47] Bai L, Conway B. Complex behavior of Al dissolution in non-aqueous Medium as revealed by impedance spectroscopy. J Electrochem Soc 1990;137:3737–47.
[48] Mandai T, Johansson P. A challenge for rechargeable Al-batteries: $AlCl_3$-free deep eutectic solvent and cationic solvate based electrolytes. Meet Abstr 2016;MA2016–03:1144.
[49] Ferrara C, Dall'Asta V, Berbenni V, Quartarone E, Mustarelli P. Physicochemical characterization of $AlCl_3$–1-Ethyl-3-methylimidazolium chloride ionic liquid electrolytes for aluminum rechargeable batteries. J Phys Chem C 2017;121:26607–14.
[50] Gálová M. Electrodeposition of aluminium from organic aprotic solvents. Surf Technol 1980;11:357–69.
[51] Graef M. The mechanism of aluminum electrodeposition from solutions of $AlCl_3$ and $LiAlH_4$ in THF. J Electrochem Soc 1985;132:1038–46.
[52] Wilkes J. Molten salts and ionic liquids - are they not the same thing. ECS Transactions 2007;3:3–7.
[53] Arnett E, Wolf J. An electrochemical Scrutiny of Organometallic iron Complexes and Hexamethylbenzene in a room temperature molten salt. J Am Chem Soc 1975;97:3264–5.
[54] Gale R, Gilbert B, Osteryoung R. Raman Spectra of molten aluminum chloride: 1-butylpyridinium chloride systems at ambient temperatures. Inorg Chem 1978;17:2728–9.
[55] Robinson J, Osteryoung R. An electrochemical and spectroscopic study of some Aromatic Hydrocarbons in the room temperature molten salt system Aluminium chloride-n-butyl Pyridinium chloride. J Am Chem Soc 1979;101:323–7.
[56] Jiang T, Chollier Brym MJ, Dubé G, Lasia A, Brisard GM. Electrodeposition of aluminium from ionic liquids: Part I—electrodeposition and surface morphology of aluminium from aluminium chloride ($AlCl_3$)–1-ethyl-3-methylimidazolium chloride ([EMIm]Cl) ionic liquids. Surf Coating Technol 2006;201:1–9.
[57] Wilkes J, Zarowotko M. Air and water stable 1-Ethyl-3-methylimidazolium based ionic liquids. J Chem Soc 1992;0:965–7.
[58] Wilkes J, Levisky J, Wilson R, Hussey C. Dialkylimidazolium chloroaluminate melts: a new Class of room temperature ionic liquids for electrochemistry, spectroscopy, and synthesis. Inorg Chem 1982;21:1263–4.
[59] Wilkes J, Hussey C. Selection of cations for Ambient temperature chloroaluminate molten salts using MNDO molecular Orbital Calculations. Springfield, Virginia: Frank J. Seiler Research Laboratory; 1982.
[60] Jones S, Blomgren G. Low-temperature molten salt electrolytes based on Aralkyl Quaternary or Ternary Onium salts. J Electrochem Soc 1989;136:424–7.
[61] National Center for Biotechnology Information. 1-Ethyl-3-Methylimidazolium.
[62] Zhang M, Kamavaram V, Reddy R. New electrolytes for aluminum production: ionic liquids. JOM 2003;55:54–7.
[63] Chakrabarti MH, Mjalli FS, AlNashef IM, Hashim MA, Hussain MA, Bahadori L, et al. Prospects of applying ionic liquids and deep eutectic solvents for renewable energy storage by means of redox flow batteries. Renew Sustain Energy Rev 2014;30:254–70.
[64] Endres F. Ionic liquids: solvents for the electrodeposition of metals and semiconductors. ChemPhysChem 2002;3:144–54.
[65] Cooper E, Andrews C, Wheatley P, Webb P, Wormald P, Morris R. Ionic liquids and eutectic mixtures as solvent and template in synthesis of zeolite analogues. Nature 2004;430:1012–5.
[66] Alhaji A. Electrodeposition of Alloys from deep eutectic solvents. University of Leicester; 2011.
[67] Zhao Y, VanderNoot T. Electrodeposition of aluminium from room temperature $AlCl_3$-TMPAC molten salts. Electrochemica Acta 1997;42:1639–43.
[68] Poetz S, Handel P, Fauler G, Fuchsbichler B, Schmuck M, Koller S. Evaluation of decomposition products of EMImCl·1.5$AlCl_3$ during aluminium electrodeposition with different analytical methods. Royal Society of Chemistry 2014;4:6685–90.
[69] Abbott AP, Frisch G, Hartley J, Karim WO, Ryder KS. Anodic dissolution of metals in ionic liquids. Prog Nat Sci: Materials International 2015;25:595–602.
[70] Xia S, Zhang X-M, Huang K, Chen Y-L, Wu Y-T. Ionic liquid electrolytes for aluminium secondary battery: influence of organic solvents. J Electroanal Chem 2015;757:167–75.
[71] Popolo MD, Voth G. On the structure and dynamics of ionic liquids. J Phys Chem B 2004;108:1744–52.
[72] Gifford P, Palmisano J. An aluminum/chlorine rechargeable cell Employing a room temperature molten salt electrolyte. J Electrochem Soc 1988;135:650–4.
[73] Melton T, Joyce J, Maloy J, Boon J, Wilkes J. Electrochemical studies of sodium chloride as a Lewis buffer for room temperature chloroaluminate molten salts. J Electrochem Soc 1990;137:3865–9.
[74] Brown TL, LeMay HE, Bursten BE, Murphy C, Woodward P, Langford S, et al. Chemistry: the central Science. Pearson Higher Education AU; 2013.
[75] Stadie NP, Wang S, Kravchyk KV, Kovalenko MV. Zeolite-templated carbon as an ordered microporous electrode for aluminum batteries. ACS Nano 2017;11:1911–9.
[76] Lloyd D, Vainikka T, Kontturi K. The development of an all copper hybrid redox flow battery using deep eutectic solvents. Electrochim Acta 2013;100:18–23.
[77] Mecerreyes D. Polymeric ionic liquids: Broadening the properties and applications of polyelectrolytes. Prog Polym Sci 2011;36:1629–48.

[78] Chaurasia SK, Singh RK, Chandra S. Structural and transport studies on polymeric membranes of PEO containing ionic liquid, EMIM-TY: evidence of complexation. Solid State Ionics 2011;183:32–9.
[79] Luo S, Zhang S, Wang Y, Xia A, Zhang G, Du X, et al. Complexes of ionic liquids with poly(ethylene glycol)s. J Org Chem 2010;75:1888–91.
[80] Schoetz T, Ponce de Leon C, Bund A, Ueda M. Electro-polymerisation and characterisation of PEDOT in Lewis basic, neutral and acidic EMImCl-$AlCl_3$ ionic liquid. Electrochim Acta 2018;263:176–83.
[81] Angell CA, Liu C, Sanchez E. Rubbery solid electrolytes with dominant cationic transport and high ambient conductivity. Nature 1993;362:137–9.
[82] Schoetz T, Leung O, Ponce de Leon C, Zaleski C, Efimov I. Aluminium deposition in EMImCl-AlCl3 ionic liquid and Ionogel for improved aluminium batteries. J Electrochem Soc 2020;167.
[83] Boisset A, Jacquemin J, Anouti M. Physical properties of a new Deep Eutectic Solvent based on lithium bis[(trifluoromethyl)sulfonyl]imide and N-methylacetamide as superionic suitable electrolyte for lithium ion batteries and electric double layer capacitors. Electrochim Acta 2013;102:120–6.
[84] Paiva A, Craveiro R, Aroso I, Martins M, Reis RL, Duarte ARC. Natural deep eutectic solvents – solvents for the 21st Century. ACS Sustainable Chem Eng 2014;2:1063–71.
[85] Zhang C, Ding Y, Zhang L, Wang X, Zhao Y, Zhang X, et al. A sustainable redox-flow battery with an aluminum-based, deep-eutectic-solvent Anolyte. Angew Chem Int Ed Engl 2017;56:7454–9.
[86] Smith EL, Abbott AP, Ryder KS. Deep eutectic solvents (DESs) and their applications. Chem Rev 2014;114:11060–82.
[87] Abbott A, Harris R, Hsieh Y, Ryder K, Sun I. Aluminium electrodeposition under ambient conditions. Royal Society of Chemistry 2014;16.
[88] Fang Y, Yoshii K, Jiang X, Sun X-G, Tsuda T, Mehio N, et al. An AlCl3 based ionic liquid with a neutral substituted pyridine ligand for electrochemical deposition of aluminum. Electrochim Acta 2015;160:82–8.
[89] Li M, Gao B, Liu C, Chen W, Shi Z, Hu X, et al. Electrodeposition of aluminum from $AlCl_3$/acetamide eutectic solvent. Electrochim Acta 2015;180:811–4.
[90] Zhang L, Zhang C, Ding Y, Ramirez-Meyers K, Yu G. A low-cost and high-energy hybrid iron-aluminum liquid battery achieved by deep eutectic solvents. Joule 2017;1:623–33.
[91] Abbott AP, Alhaji AI, Ryder KS, Horne M, Rodopoulos T. Electrodeposition of copper–tin alloys using deep eutectic solvents. Transactions of the IMF 2016;94:104–13.
[92] Feibelman PJ. Diffusion path for an Al adatom on Al(001). Phys Rev Lett 1990;65:729–32.
[93] Jackle M, Gross A. Microscopic properties of lithium, sodium, and magnesium battery anode materials related to possible dendrite growth. J Chem Phys 2014;141:174710.
[94] Barton J, Bockris J. The electrolytic growth of dendrites from ionic solutions. Proceedings of the Royal Society 1962;268:485–505.
[95] Schoetz T. Preparation and Characterisation of an aluminium-conductive polymer battery in a chloroaluminate ionic liquids for future energy storage. University of Southampton; 2019.
[96] Hjuler H. A novel Inorganic low melting electrolyte for secondary aluminium-nickel sulfide batteries. J Electrochem Soc 1989;136:901–6.
[97] Legrand L, Chassaing E, Chausse A, Messina R. RDE and impedance study of anodic dissolution of aluminium in organic $AlCl_3$/dimethylsulfone electrolytes. Electrochemica Acta 1998;43:3109–15.
[98] Chen C, Tsong TT. Displacement distribution and atomic jump direction in diffusion of Ir atoms on the Ir(001) surface. Phys Rev Lett 1990;64:3147–50.
[99] Kellogg GL, Feibelman PJ. Surface self-diffusion on Pt(001) by an atomic exchange mechanism. Phys Rev Lett 1990;64:3143–6.
[100] Henkelman G, Jonsson H. Multiple time scale simulations of metal crystal growth reveal the importance of multiatom surface processes. Phys Rev Lett 2003;90:116101.
[101] Matsui M. Study on electrochemically deposited Mg metal. J Power Sources 2011;196:7048–55.
[102] Li R, Zhong Y, Huang C, Tao X, Ouyang Y. Surface energy and surface self-diffusion of Al calculated by embedded atom method. Phys B Condens Matter 2013;422:51–5.
[103] Harbick B, Suh L, Fong J. Closest packed structures. Chem Libretexts; 2017.
[104] Born M. On the stability of crystal lattices. I. Mathematical Proceedings of the Cambridge Philosophical Society 2008;36.
[105] Zhang J-G, Xu W, Henderson WA. Characterization and modeling of lithium dendrite growth. Lithium metal anodes and rechargeable lithium metal Batteries2017. p. 5-43.
[106] Pradhan D, Reddy RG. Mechanistic study of Al electrodeposition from EMIC–$AlCl_3$ and BMIC–$AlCl_3$ electrolytes at low temperature. Mater Chem Phys 2014;143:564–9.
[107] Carlin R, Crawford W, Bersch M. Nucleation and morphology studies of aluminum deposited from an ambient-temperature chloroaluminate molten salt. J Electrochem Soc 1992;139:2720–7.
[108] Allongue P, Souteyrand E. Metal electrodeposition on semiconductors Part I. Comparison with glassy carbon in the case of platinum deposition. J Electroanal Chem 1990;286:217–37.
[109] Auborn J, Barberio Y. An ambient temperature secondary aluminum electrode: its cycling rates and its cycling efficiencies. J Electrochem Soc 1985;132:598–601.
[110] Peled E, Gileadi E. The electrodeposition of aluminum from Aromatic Hydrocarbon - 1. Composition of Baths and the effect of additives. J Electrochem Soc 1976;123:15–9.
[111] Dumas P, Dubarry-Barbe JP, Rivière D, Levy Y, Corset J. Growth of Thin Alumina film on aluminium at room temperature : a kinetic and spectroscopic study by surface Plasmon Excitation. J Phys Colloq 1983;44. C10-205-C10-8.
[112] Böttcher R, Mai S, Ispas A, Bund A. Aluminum deposition and dissolution in [EMIm]Cl-based ionic liquids–kinetics of charge–transfer and the rate–Determining step. J Electrochem Soc 2020:167.
[113] Paranthaman M, Brown G, Nanda XS, Manthiram A, Manivannan A. A transformational, high energy density secondary Aluminum ion battery. 218th ECS Meeting: The Electrochemical Society; 2010.
[114] Wang S, Kravchyk KV, Krumeich F, Kovalenko MV. Kish graphite flakes as a cathode material for an aluminum chloride-graphite battery. ACS Appl Mater Interfaces 2017;9:28478–85.
[115] Wang H, Bai Y, Chen S, Luo X, Wu C, Wu F, et al. Binder-free V_2O_5 cathode for greener rechargeable aluminum battery. ACS Appl Mater Interfaces 2015;7:80–4.
[116] Gao T, Li X, Wang X, Hu J, Han F, Fan X, et al. A rechargeable Al/S battery with an ionic-liquid electrolyte. Angew Chem Int Ed Engl 2016;55:9898–901.
[117] Wang S, Yu Z, Tu J, Wang J, Tian D, Liu Y, et al. A novel aluminum-ion battery: Al/$AlCl_3$-[EMIm]Cl/Ni_3S_2@Graphene. Advanced Energy Materials 2016;6:1600137.
[118] Rani JV, Kanakaiah V, Dadmal T, Rao MS, Bhavanarushi S. Fluorinated natural graphite cathode for rechargeable ionic liquid based aluminum-ion battery. J Electrochem Soc 2013;160:A1781–4.
[119] Elia GA, Hasa I, Greco G, Diemant T, Marquardt K, Hoeppner K, et al. Insights into the reversibility of aluminum graphite batteries. J Mater Chem 2017;5:9682–90.
[120] Wang DY, Wei CY, Lin MC, Pan CJ, Chou HL, Chen HA, et al. Advanced rechargeable aluminium ion battery with a high-quality natural graphite cathode. Nat Commun 2017;8:14283.
[121] Chen H, Cong TN, Yang W, Tan C, Li Y, Ding Y. Progress in electrical energy storage system: a critical review. Prog Nat Sci 2009;19:291–312.
[122] Agiorgousis ML, Sun Y-Y, Zhang S. The role of ionic liquid electrolyte in an aluminum–graphite electrochemical cell. ACS Energy Letters 2017;2:689–93.
[123] Juza R, Seidel H. Zur Kenntnis des Chlorgraphits. Z Anorg Allg Chem 1962;317:73–83.
[124] Wu MS, Xu B, Chen LQ, Ouyang CY. Geometry and fast diffusion of $AlCl_4$ cluster intercalated in graphite. Electrochim Acta 2016;195:158–65.
[125] Gao Y, Zhu C, Chen Z, Lu G. Understanding ultrafast rechargeable aluminum-ion battery from first-Principles. J Phys Chem C 2017;121:7131–8.
[126] Bhauriyal P, Mahata A, Pathak B. The staging mechanism of $AlCl_4$ intercalation in a graphite electrode for an aluminium-ion battery. Phys Chem Chem Phys 2017;19:7980–9.
[127] Jung SC, Kang Y-J, Yoo D-J, Choi JW, Han Y-K. Flexible few-layered graphene for the ultrafast rechargeable aluminum-ion battery. J Phys Chem C 2016;120:13384–9.
[128] Bhauriyal P, Mahata A, Pathak B. A computational study of a single-walled carbon-nanotube-based ultrafast high-capacity aluminum battery. Chem Asian J 2017;12:1944–51.
[129] Shirakawa H, Louis E, Macdiarmid A, Chiang C, Heeger A. Synthesis of electrically conducting organic polymers: Halogen Derivatives of polyacetylene, $(CH)_x$. JCS Chem Comm 1977:578.
[130] Jagur-Grodzinski J. Electronically conductive polymers. Polym Adv Technol 2002;13:615–25.
[131] Salzner U. Electronic structure of conducting organic polymers: insights from time-dependent density functional theory. Comput Mol Sci 2014;4:601–22.
[132] Rajesh M, Raj CJ, Manikandan R, Kim BC, Park SY, Yu KH. A high performance PEDOT/PEDOT symmetric supercapacitor by facile in-situ hydrothermal polymerization of PEDOT nanostructures on flexible carbon fibre cloth electrodes. Materials Today Energy 2017;6:96–104.
[133] Brédas J, Street G. Polarons, Bipolarons, and Solitons in conducting polymers. Acc Chem Res 1985;18:309–15.
[134] Kertesz M, Choi CH, Yang S. Conjugated polymers and aromaticity. Chem Rev 2005;105:3448–81.
[135] Heeger AJ, Kivelson S, Schrieffer JR, Su WP. Solitons in conducting polymers. Rev Mod Phys 1988;60:781–850.
[136] Tautz R, Da Como E, Limmer T, Feldmann J, Egelhaaf HJ, von Hauff E, et al. Structural correlations in the generation of polaron pairs in low-bandgap polymers for photovoltaics. Nat Commun 2012;3:970.
[137] Craig B, Skylaris C-K, Schoetz T, Ponce de Leon C. A computational chemistry approach to modelling conducting polymers in ionic liquids for next generation batteries. Energy Rep 2017;6(5):198–208.
[138] Heinze J, Frontana-Uribe B, Ludwigs S. Electrochemistry of conducting polymers - Persistent models and new concepts. Chem Rev 2010;110:4724–71.
[139] Shekaari H, Zafarani-Moattar MT, Niknam M. Thermodynamic evaluation of imidazolium based ionic liquids with thiocyanate anion as effective solvent to thiophene extraction. J Mol Liq 2016;219:975–84.
[140] Wu X, Kang F, Duan W, Li J. Density functional theory calculations: a powerful tool to simulate and design high-performance energy storage and conversion materials. Prog Nat Sci: Materials International 2019;29(3):247–55.
[141] Freund M, Svenda S, Deore B. In situ polymerization of conducting poly(3,4-ethylene dioxythiophene). In: Office USPaT, editor. US: University of Manatoba; 2012.
[142] Dietrich M, Heinze J, Heywang G, Jonas F. Electrochemical and spectroscopic characterization of polyalkylenedioxythiophenes. J Electroanal Chem 1994;369:87–92.
[143] Demtchenko S, Tarr NG, McGarry S. Effect of PEDOT band structure on conductive polymer-insulator-silicon junctions. J Appl Phys 2017;122.

[144] Schoetz T, Ponce de Leon C, Bund A, Ueda M. Electro-polymerisation of 3,4-ethylenedioxythiophene on reticulated vitreous carbon in imidazolium-based chloroaluminate ionic liquid as energy storage material. Electrochem Commun 2018;89:52–6.
[145] Sun K, Zhang S, Li P, Xia Y, Zhang X, Du D, et al. Review on application of PEDOTs and PEDOT:PSS in energy conversion and storage devices. J Mater Sci Mater Electron 2015;26:4438–62.
[146] Roncali J, Blanchard P, Frère P. 3,4-Ethylenedioxythiophene (EDOT) as a versatile building block for advanced functional π-conjugated systems. J Mater Chem 2005;15:1589–610.
[147] Groenendaal L, Jonas F, Freitag D, Pielartzik H, Reynolds J. Poly(3,4-ethylenedioxythiophene) and its Derivatives: past, present, and future. Adv Mat 2000;12:481–94.
[148] Schoetz T, Kurniawan M, Stich M, Peipmann R, Efimov I, Ispas A, et al. Understanding the charge storage mechanism of conductive polymers as hybrid battery-capacitor materials in ionic liquids by in situ atomic force microscopy and electrochemical quartz crystal microbalance studies. J Mater Chem 2018;6:17787–99.
[149] Reed LD, Menke E. The Roles of V_2O_5 and stainless steel in rechargeable Al-ion batteries. J Electrochem Soc 2013;160:A915–7.
[150] Liu Y, Sang S, Wu Q, Lu Z, Liu K, Liu H. The electrochemical behavior of Cl − assisted Al 3+ insertion into titanium dioxide nanotube arrays in aqueous solution for aluminum ion batteries. Electrochim Acta 2014;143:340–6.
[151] Koketsu T, Ma J, Morgan BJ, Body M, Legein C, Dachraoui W, et al. Reversible magnesium and aluminium ions insertion in cation-deficient anatase TiO2. Nat Mater 2017;16:1142–8.
[152] Cohn G, Ma L, Archer LA. A novel non-aqueous aluminum sulfur battery. J Power Sources 2015;283:416–22.
[153] Yu X, Manthiram A. Electrochemical energy storage with a reversible nonaqueous room-temperature aluminum-sulfur chemistry. Advanced Energy Materials 2017;7.
[154] Yu X, Boyer MJ, Hwang GS, Manthiram A. Room-temperature aluminum-sulfur batteries with a lithium-ion-Mediated ionic liquid electrolyte. Inside Chem 2018;4:586–98.
[155] Le D, Passerini S, Coustier F, Guo J, Soderstrom T, Owens B, et al. Intercalation of polyvalent cations into V_2O_5 aerogels. Chem Mater 1998;10:682–4.
[156] Jayaprakash N, Das SK, Archer LA. The rechargeable aluminum-ion battery. Chem Commun (Camb) 2011;47:12610–2.
[157] Chiku M, Takeda H, Matsumura S, Higuchi E, Inoue H. Amorphous vanadium oxide/carbon composite positive electrode for rechargeable aluminum battery. ACS Appl Mater Interfaces 2015;7:24385–9.
[158] Yu SH, Feng X, Zhang N, Seok J, Abruna HD. Understanding conversion-type electrodes for lithium rechargeable batteries. Acc Chem Res 2018;51:273–81.
[159] Bitenc J, Lindahl N, Vizintin A, Abdelhamid ME, Dominko R, Johansson P. Concept and electrochemical mechanism of an Al metal anode – organic cathode battery. Energy Storage Materials 2019;24:379–83.
[160] Song Z, Zhan H, Zhou Y. Anthraquinone based polymer as high performance cathode material for rechargeable lithium batteries. Chem Commun (Camb). 2009:448–50.
[161] Zhang M, Watson JS, Counce RM, Trulove PC, Zawodzinski TA. Electrochemistry and morphology studies of aluminum plating/stripping in a chloroaluminate ionic liquid on porous carbon materials. J Electrochem Soc 2014;161:D163–7.